

**An-Najah National University**

**Faculty of Graduate Studies**

**Preparation of multicomponent nanoparticles for  
effective anti-inflammatory therapy**

**By**

**Nihal Ziad Izzat Zohud**

**Supervisor**

**Dr. Mohyeddin Assali**

**This Thesis is Submitted in Partial Fulfillment of the Requirements for  
the Degree of Master in Pharmaceutical Sciences, Faculty of Graduate  
Studies, An-Najah National University, Nablus - Palestine.**

**2020**

**Preparation of multicomponent nanoparticles for effective  
anti-inflammatory therapy**

**By**

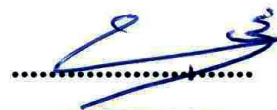
**Nihal Ziad Izzat Zohud**

**This Thesis was defended successfully on 23/8/2020 and approved by:**

**Defense Committee Members**

**Signature**

**1. Dr. Mohyeddin Assali / Supervisor**

A handwritten signature in blue ink, appearing to be 'Mohyeddin', written over a dotted line.

**3. Dr. Hani Shtaya / External Examiner**

A handwritten signature in blue ink, appearing to be 'Hani', written over a dotted line.

**4. Dr. Ahed Zyoud / Internal Examiner**

A handwritten signature in blue ink, appearing to be 'Ahed Zyoud', written over a dotted line.

## **Dedication**

It is dedicated with gratitude to

My backbone (Mum and Dad) whose strength and confidence inspired me  
to continue and never give up till reach.

...The biggest blessing I have is your presence...

To my beloved sister Manar and brothers who shared me childhood  
memories and grown-up dreams. My precious family members, may Allah  
bless and keep you.

To anyone who left a distinguished fingerprint in his/her life

## **Acknowledgement**

My praise and thanks first and foremost to great Allah for gifting me the power, determination and patience to carry out and complete this thesis.

All thanks and appreciation to my supervisor Dr. Mohyeddin Assali for his superb dealing with us as he did not spare any time or effort to mentor me.

All thanks and gratitude to the rest of examination committee for reading my thesis, their insightful comments and suggestions and invaluable criticisms.

Thanks to Hamdi Mango Center, Faculty of Medicine and Faculty of Science at the Jordan University for their assistance in NMR, and TEM measurements.

Special and deepest thanks to the staff of the laboratories of the College of Pharmacy, Science and Medicine for providing help and assistance, especially the supervisors of the laboratories of the College of Pharmacy Mr. Mohammad Arar and the lab workers Tahreer Shtayeh, Linda Arar and Noura Ghazal.

My friends and colleagues at the Faculty of higher graduates and Pharmacy deserve special thanks for their assistance, support and for the funniest time that we spent together during the period of my study.

I would like to declare my deep, sincere appreciation, love and gratitude to my family beginning with my mother and father and ending with my sister and brothers. This work could not be completed without your endless love, encouragement, helping and support.

٧  
الإقرار

أنا الموقع أدناه موقع الرسالة التي تحمل العنوان:

**"Preparation of multicomponent nanoparticles for effective anti-inflammatory therapy"**

أقر بأن ما اشتملت عليه الرسالة هو نتاج جهدي الخاص، باستثناء ما تمت الإشارة إليه حيثما ورد، وأن هذه الرسالة ككل، أو أي جزء منها لم يقدم من قبل لنيل أي درجة أو لقب علمي أو بحثي لدى أي مؤسسة تعليمية أو بحثية أخرى.

**Declaration**

The work provided in this thesis, unless otherwise referenced was the researcher's own work, and has not been submitted elsewhere for any other degree or qualification.

Student's name:

اسم الطالب: نهال زينا محمد زهد

Signature:



التوقيع:

Date:

23/08/2020

التاريخ

## List of Contents

No	Content	Pages
	Dedication	iii
	Acknowledgement	iv
	Declaration	v
	List of Tables	viii
	List of Figures	ix
	List of Schemes	x
	List of Abbreviations	xi
	Abstract	xiii
	<b>Chapter One: Introduction</b>	1
1.1	Inflammation	1
1.2	Cyclooxygenases and inflammation	1
1.3	Non-steroidal anti-inflammatory drugs (NSAIDs)	2
1.4	Indomethacin	4
1.5	Famotidine	6
1.6	Paracetamol	6
1.7	Multi-component delivery systems	7
1.8	Nanotechnology and Nanoparticles	8
1.8.1	Biodegradable polymers	9
1.9	Polymeric nanoparticles preparation methods	11
1.9.1	Nanoprecipitation	12
1.10	Nanoemulsion	13
1.10.1	High energy methods	14
1.11	Literature review	15
	Aim of the study	19
	Objectives	20
	<b>Chapter Two: Reagents and methodology</b>	21
2.1	Reagents and materials	21
2.1.1	Co-drug synthesis reagents	21
2.1.2	Analysis reagents and chemicals	21
2.1.3	Nanoemulsions and polymeric nanoparticles preparations reagents	22
2.1.4	Release and stability studies reagents	22
2.1.5	Biology tests reagents	23
2.2	Instrumentations	23
2.3	Preparation of the buffers	24
2.4	Methodology	25
2.4.1	Synthesis and characterization of IND-PAR Co-drug	25
2.4.2	Preparation of nanoemulsions	26

2.4.4	Preparation of polymeric nanoparticles	27
2.4.5	Encapsulating Co-NE into FAM-PNPs	27
2.4.6	HPLC analytical method development	28
2.4.7	In vitro release studies	32
2.4.8	Drug release kinetics	33
2.4.9	Stability studies	33
2.4.10	Cell biocompatibility tests	34
	<b>Chapter three: Results and discussion</b>	36
3.1	Synthesis of IND-PAR Co-drug	36
3.2	Preparation of nanoemulsion	37
3.3	Preparation of polymeric nanoparticles	39
3.4	Encapsulating Co-NE into FAM-polymeric nanoparticles	40
3.5	HPLC analytical method development	42
3.5.1	Method development	42
3.5.2	Method validation	43
3.6	Encapsulation efficiency (EE)	49
3.7	In vitro release studies	50
3.7.2	In vitro release of Co-drug and FAM without PLE	51
3.8	Drug release kinetics	52
3.9	Stability studies	54
3.9.1	Stability studies at different temperatures	54
3.9.2	Stability studies using different buffers	55
3.10	Cellular biocompatibility test	56
	Conclusion	58
	References	59
	Appendix	83
	Appendix A: RP-HPLC Method Development and Validation of Synthesized Codrug in Combination with Indomethacin, Paracetamol, and Famotidine article	83
	الملخص	ب

**List of Table**

<b>NO.</b>	<b>Table title</b>	<b>Page</b>
1	Summary of method development optimization.	29
2	Robustness parameters and conditions checked.	31
3	Characterization of blank and Co@NEs.	38
4	Characterization of PNPs	39
5	Characterization of PLGA and PCL nanosystems.	42
6	The HPLC chromatographic conditions.	43
7	The accuracy results in the conc. range (0.08-0.12) mg/mL.	45
8	The precision results at different precision levels.	46
9	Results of robustness at different variable parameters.	48
10	System suitability.	49
11	EE values for Co-drug and FAM.	50
12	The most fitted models for both nanosystems.	54
13	Stability study at different temperatures.	55
14	Stability studies using acidic and alkaline buffers.	56



## List of Figure

<b>NO.</b>	<b>Figure title</b>	<b>Page</b>
1.1	Inflammation process and NSAIDs targeted sites.	2
1.2	Indomethacin structure.	5
1.3	Paracetamol structure.	7
1.4	Nanoprecipitation method.	13
1.5	Ultrasonication technique.	15
3.1	TEM image showed the morphology of the formed nanoemulsion.	38
3.2	TEM images of both nanosystems <b>A)</b> Co-NE@PCL and <b>B)</b> Co-NE@PLGA nanoparticles.	41
3.3	Chromatogram of the eluted peaks for the component mixture.	43
3.4	Linearity curves for the four compounds.	44
3.5	Chromatogram of the eluted peaks for the component mixture with the inactive ingredients.	45
3.6	Chromatogram of System suitability.	49
3.7	% Conversion of Co-drug. A) % Conversion of free Co-drug, B) % Conversion of Co-NE, C) % Conversion of Co-NE@PLGA NPs and D) % Conversion of Co-NE@PCL NPs.	51
3.8	% Release of Co-drug and FAM. A) PLGA nanosystem, B) PCL nanosystem.	52
3.9	Viability assay of Co-NE@PCL and Co-NE@PLGA nanoparticles incubated with <b>A)</b> HeLa cells; <b>B)</b> 3T3 fibroblast.	57

**List of Schemes**

<b>NO.</b>	<b>Scheme title</b>	<b>Page</b>
<b>1</b>	Schematic representation of the encapsulation of NSAIDs into controlled-release microcapsules.	18
<b>2</b>	Synthetic scheme of Co-drug.	36
<b>3</b>	Schematic representation of the whole nanosystem.	40

## List of Abbreviations

<b>Symbol</b>	<b>Abbreviation</b>
<b>ACN</b>	Acetonitrile
<b>AIC</b>	Akaike Information Criterion
<b>Aq.</b>	Aqueous
<b>AS</b>	Ankylosing spondylitis
<b>Av.</b>	Average
<b>Cat. #</b>	Catalog number
<b>CDI</b>	Carbonyl diimidazole
<b>CGM</b>	Cell-culture growth media
<b>CNS</b>	Central Nervous System
<b>Conc.</b>	Concentration
<b>COX</b>	Cyclooxygenase
<b>DLS</b>	Dynamic Light Scattering
<b>DMAP</b>	4-Dimethylaminopyridine
<b>DSC</b>	Differential Scanning Calorimetry
<b>EDC</b>	N-(3-Dimethylaminopropyl)-N'-ethylcarbodiimide hydrochloride
<b>EtOAc</b>	Ethyl acetate
<b>FAM</b>	Famotidine
<b>FBS</b>	Fetal bovine serum
<b>GERD</b>	Gastroesophageal Reflux
<b>GI</b>	Gastrointestinal
<b>h.</b>	Hour/s
<b>Hex</b>	Hexane
<b>HLB</b>	Hydrophilic-lipophilic balance
<b>HRMS</b>	High-resolution mass spectrometry
<b>IND</b>	Indomethacin
<b>LOD</b>	Limit of Detection
<b>LOQ</b>	Limit of Quantification
<b>MeOH</b>	Methanol
<b>Mix.</b>	Mixture
<b>MSC</b>	Model Selection Criterion
<b>MTS</b>	3-(4,5-dimethylthiazol-2-yl)-5-(3-carboxymethoxyphenyl)-2-(4-sulfophenyl)-2H-tetrazolium
<b>MPS</b>	Mononuclear Phagocyte System
<b>MW</b>	Molecular weight
<b>NaHCO<sub>3</sub></b>	Sodium bicarbonate

<b>NC</b>	Nanocapsule
<b>NE</b>	Nanoemulsion
<b>NMR</b>	Nuclear Magnetic Resonance
<b>NPs</b>	Nanoparticles
<b>NSAIDs</b>	Non-steroidal anti-inflammatory drugs
<b>°C</b>	Degree Celsius
<b>o/w</b>	Oil-in-water
<b>PAR</b>	Paracetamol
<b>PBS</b>	Phosphate buffer saline
<b>PCL</b>	Polycaprolactone
<b>PDLA</b>	Poly D-Lactide
<b>PDLLA</b>	Poly (D,L-lactide)
<b>PEG</b>	Polyethylene glycol
<b>Pen-Strep</b>	Penicillin-streptomycin
<b>PFA</b>	Paraformaldehyde
<b>PGA</b>	Polyglycolic acid
<b>PGs</b>	Prostaglandins
<b>Ph</b>	Power of hydrogen
<b>PLA</b>	Polylactide
<b>PLE</b>	Porcine Liver Enzyme
<b>PLGA</b>	Poly (D,L-lactide-co-glycolide)
<b>PLLA</b>	Poly L-Lactide
<b>PMAM</b>	Polyamidoamine
<b>PNPs</b>	Polymeric nanoparticles
<b>POE</b>	Polyoxyethylene
<b>PPI</b>	Proton Pump Inhibitors
<b>PVA</b>	Polyvinyl alcohol
<b>RA</b>	Rheumatoid Arthritis
<b>RP-HPLC</b>	Reverse phase- High Pressure Liquid Chromatography
<b>RPMI</b>	Roswell Park Memorial Institute
<b>RSD</b>	Relative Standard Deviation
<b>SEM</b>	Scanning Electron Microscope
<b>S/N</b>	Signal to noise ratio
<b>SMP</b>	Shape-memory Polymers
<b>TEM</b>	Transmission Electron Microscope
<b>T</b>	Temperature
<b>w/o</b>	Water-in-oil
<b>UV-vis</b>	Ultraviolet-visible
<b>XRD</b>	X-ray Diffraction
<b>ζ-potential</b>	Zeta potential

**Preparation of multicomponent nanoparticles for effective  
anti-inflammatory therapy**

**By**

**Nihal Ziad Izzat Zohud**

**Supervisor**

**Dr. Mohyeddin Assali**

**Abstract**

**Background:** Non-steroidal anti-inflammatory drugs are amongst the major common and widely prescribed drugs for pain and inflammation. However, their notoriety of causing gastrointestinal effects, their low water solubilities and their short half-lives would affect the patient compliance and the oral absorption of them and accordingly justify the need to have NSAIDs with controlled and sustained release manner in combination with anti-ulcer drugs. Recently, nanoparticles technology is considered an ingenious technique to overcome these drawbacks. Herein, we developed multi-drug delivery nanosystems of Indomethacin, Paracetamol and Famotidine using nanoemulsion and polymeric nanoparticles techniques.

**Methodology:** Starting from the synthesis of the Co-drug of Indomethacin and Paracetamol joined through a hydrolysable ester followed by pre-loading this Co-drug into nanoemulsion (Co-NE) which would be loaded into different polymeric nanoparticles having Famotidine utilizing nanoprecipitation approach. The developed nanosystems were characterized by transmission electron microscopy, dynamic light scattering and zeta potential analysis. Moreover, stability and biocompatibility studies were tested. In addition, a novel RP-HPLC method

was developed and validated according to ICH guidelines to study the *in vitro* release profiles of the loaded drugs (FAM and Co-drug).

**Results:** These developed nanosystems showed a hydrodynamic size between 190-240 nm and the zeta potential values ranges from -30 to -48 mV. TEM images confirmed Co-NE loading into different polymeric nanoparticles. Stability studies revealed that these nanosystems were stable at different temperatures and buffered conditions over one month. Moreover, improvement of the solubilities of these three drugs using this encapsulation technique leading to have controlled-release multi component systems of both Co-drug and Famotidine over three days. In addition to quantification of the four drugs on one HPLC run by developing and validating a RP-HPLC method that was successfully utilized for quantification of the *in vitro* hydrolysis, release, loading and conversion of Co-drug.

**Conclusion:** These multi component nanoparticles might be a potential platform to overcome the obstacles of NSAIDs, synergize drugs with different mechanism of actions by co-encapsulating a small-sized nanoemulsion into different polymeric nanocarriers for reaching the goal of effective anti-inflammatory therapy.

# **Chapter One**

## **Introduction**

### **1.1 Inflammation**

It is a nonspecific, natural and cellular response of tissue to multiple stimuli like infection, injury, irritants and microorganisms promoting release of different protective chemicals [1]. Among these are prostaglandins (PGs), they are hormone-like mediators that play a crucial role in the inflammatory processes [2]. Heat, swelling, redness and pain are four key markers of inflammation which can be due to different disease e.g.; cancer, arthritis, infection, neurodegenerative and cardiovascular diseases [3, 4]. Inflammation is an essential status leading to the elimination of insulting factors and rejuvenation of tissues structure and physiological function [5].

### **1.2 Cyclooxygenases and inflammation**

Both COX isoforms: COX-1 and COX-2 are considered targeted sites of NSAIDs. In spite of both COXs found as homodimers, only one monomer is utilized for substrate binding. Therefore, NSAIDs bind one monomer of them and inactivate the COX site, resulting in terminating prostanoid formation [6]. Although COX-2 manifested to be the predominant source of PG formation during inflammation, both isoforms may contribute in acute inflammatory processes as COX-1 can be induced within lipopolysaccharide (LPS)-mediated inflammatory response and differentiation of cells [7]. COX-1 takes part in housekeeping roles such as:

gastric mucosa protection, platelet and renal homeostasis and other physiological functions by producing PGs and thromboxane A<sub>2</sub> as summarized in **Figure 1.1**. On the other hand, COX-2 produces PGs that mostly linked to inflammation and pain, so that COX-2 inhibition represents the NSAIDs' desired anti-inflammatory, analgesic and anti-pyretic implications whereas COX-1 inhibition represents the NSAIDs' undesired GI and renal side effects [8, 9].

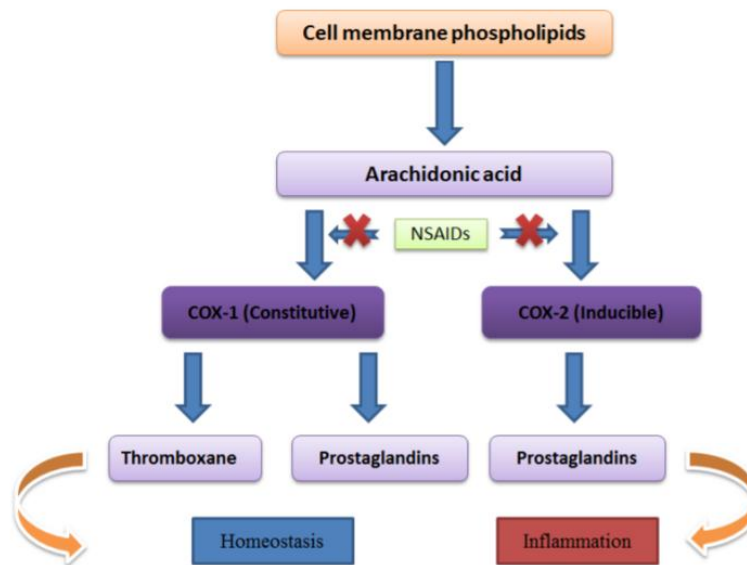


**Figure 1.1:** Inflammation process and NSAIDs targeted sites [10].

### 1.3 Non-steroidal anti-inflammatory drugs (NSAIDs)

Non-steroidal anti-inflammatory drugs (NSAIDs) are within the highest consumed and extensively prescribed drugs for both pain and inflammation throughout the world which found as over the counter medications [10, 11]. Their blockage of prostaglandins synthesis by inhibiting cyclooxygenase



(COX) is accountable for couple of the desired anti-inflammatory effects and the unpleasant gastrointestinal effects [12, 13].

They are divided into two classes in the basis of COX selectivity: nonselective NSAIDs which block both COX-1 and COX-2 and COX-2 selective inhibitors known as coxibs [14, 15]. Based on their chemical structure, NSAIDs were classified into eight groups e.g.: oxicams (piroxicam), phenylpropionic acid derivatives (ibuprofen), phenyl acetic acid derivatives (diclofenac), indoleacetic acid derivatives (indomethacin), pyrazolone derivatives (metamizol), para-aminophenol derivatives (acetaminophen) and salicylates (Aspirin) [16]. Moreover, they can be classified according to their plasma half-lives as short half-life drugs less than 6 h. such as: diclofenac, ibuprofen, indomethacin and ketorolac and also as long half-life more than 6 h. such as: sulindac, piroxicam and naproxen [17].

NSAIDs can be delivered by different route of administration: oral, topical, intramuscular, ocular and others but mostly by oral route which is considered the most efficient anti-inflammatory route. In return, it is the most causative route of gastrointestinal side effects [18]. These effects could be prevented by the use of gastropreventive agents such as H<sub>2</sub>-receptor antagonists, misoprostol and proton pump inhibitors (PPI) [19], about 20 % of elderly patients who are chronically using NSAIDs is applying this strategy [20]. Taking selective COX-2 inhibitors considered another strategy to decrease the disagreeable effects. However, using these

selective inhibitors increases the risk of cardiovascular adverse effects [21]. Thus, it is crucial to determine the best choice of GI protection for patients on chronic use of NSAIDs and tailor GI risk factors against cardiovascular risk factors [19].

NSAIDs are often prescribed in several chronic diseases e.g.: rheumatoid arthritis (RA), osteoarthritis and ankylosing spondylitis (AS) but at higher doses, they often induce large number of side effects and poor patient compliance as a consequence. Accordingly, these drugs need strict monitoring in case with patients with renal and cardiovascular diseases [22].

Generally, they are weak acids having pka ranges from 3 to 5, they are owning different variations in safety, efficacy and tolerability due to fluctuations of bioavailability and distribution in the body [23]. Most of them are well-absorbed from the GI tract with an extremely protein-bound in plasma for approximately more than 95% often to albumin [24], they are mostly metabolized in the liver through oxidation and conjugation to inactives that commonly excreted in the urine and some excreted in bile [25].

#### **1.4 Indomethacin**

Indomethacin (IND) is an example of an effective, powerful and nonselective NSAID having very effective antipyretic, analgesic and anti-inflammatory activities [26]. Its NSAID chemical classification is an indoleacetic acid derivative with the chemical name of 1-(p-

chlorobenzoyl)-5-methoxy-2-methylindole-3-acetic acid with pka 4.5 as shown in **Figure 1.2** [27]. IND is a poorly soluble class II drug with a half-life of 4-5 h inducing poor patient compliance due to multiple daily dosing [17, 28].

It is most commonly used for the treatment of inflammation resulting from rheumatoid diseases. Moreover, significant anti-cancer activities were being established against different types of cancers and many studies revealed that IND can reduce the risk of cancers especially colon by providing chemoprotective effects against tumors [29-33].

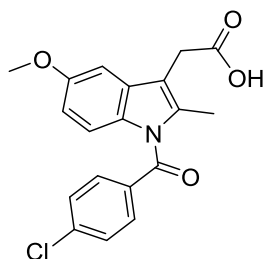


**Figure 1.2:** Indomethacin structure.

Both two COX enzymes were inhibited by IND, but COX-2 inhibition was little in comparison to COX-1. As a result, upon long-term oral administration, IND has critical complications such as: GI ulcers and renal toxicity [34].

Both its mechanism of action and undesirable physical property (poor solubility) are responsible for the GI side effects especially irritation [35, 36]. Furthermore, it can cause CNS side effects and headache considered the most frequently of these [37]. Therefore, anti-ulcer drugs such as Famotidine are co-administered to reduce the gastric side effects. In this

sense, it was noticed a strong demand for controlled release anti-inflammatory therapeutics for improving its absorption and decreasing its aforementioned side effects.

### **1.5 Famotidine**

It is a competitive histamine H-receptor antagonist (H<sub>2</sub>RA), it blocks histamine actions by binding the H-Rs which located on the parietal cells of stomach resulting in inhibition of gastric secretion [38, 39]. FAM is widely available as an OTC drug or by prescription, it is US FDA approved for the treatment of acid-related GI conditions such as: gastric and duodenal ulcers, gastroesophageal reflux disease (GERD), heartburn in adults and children with another indications for stress ulcers and pathological hypersecretory conditions [40-42]. Moreover, it is off-label used for decreasing GI complications due to NSAIDs [43].

FAM was founded to be useful for prevention on IND- induced gastric injury even in the lowest dose [44], it improves ulcer healing and reverses the GI side effects of IND by inhibiting secretion of gastric acid along with increasing collagen secretions [45, 46].

### **1.6 Paracetamol**

Recently, there has been a trend for combining NSAIDs with Paracetamol as this often provide a synergic analgesic effect and reduce the adverse effects resulting from NSAIDs [47]. Paracetamol (PAR), N-acetyl-p-aminophenol as represented in **Figure 1.3** (also recognized as

acetaminophen) is used worldwide for its analgesic and antipyretic activities. With regard to WHO pain ladder, it is considered as a first choice medication by a diversity of international guidelines for both acute and chronic pain [48, 49].

Its mechanism of action is not thoroughly understood but PAR is considered to be a weak inhibitor of PGs synthesis, its effects *in vivo* are similar to these COX-2 inhibitors, although its analgesic effects are often weaker than NSAIDs, it has better tolerance and accordingly it is often preferred [50, 51].

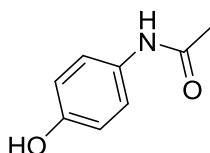


**Figure 1.3:** Paracetamol structure.

## 1.7 Multi-component delivery systems

Multi-component delivery systems would be more suitable for chronic diseases compared with conventional drug delivery systems especially for diseases like cancer, inflammatory diseases, HIV and others since they are required employing various drugs with different mechanism of actions [52-55]. In this study, therefore, we aim to design a drug delivery system that allows for controlled and sustained release of Co-drug. Furthermore, decreasing the GI side effects of IND by adding famotidine (FAM).

## **1.8 Nanotechnology and Nanoparticles**

Nanotechnology has attained prominence in unlimited fields since last century. Since it was firstly presented by Nobel laureate Richard P. Feynman over his well-known and outstanding 1959 speech “There is plenty of room at the bottom” [56], there has been great evolution in the field of nanotechnology. By nanotechnology, various types of materials were produced at nanoscale level and vast scopes of research in numerous fields were fulfilled.

Nanoparticles are a broad class of particulate dispersions or solid particles with one dimension at least with a size range from 1-100 nm [57]. Due to their small sizes, they have large surface areas which make them applicable in various fields; they exhibit exceptional physical, chemical, optical and biological characteristics at nanoscale comparable to their basic materials at higher scale. Therefore, NPs showed greater mechanical strength, stability, sensitivity and reactivity in a chemical reaction [58, 59].

They are classified into organic, inorganic and carbon based nanomaterial. Organic NPs include polymers, dendrimers, liposomes, micelles etc. Inorganic are metal and metal oxide based NPs and carbon based NPs are totally carbon and they are often classified into fullerenes, grapheme, carbon nanotubes (CNTs), carbon nanofiber and carbon black. Due to their incredible properties, NPs have been applied into different fields: electronics, drug and gene delivery, cosmetics, medicine, food, construction, environmental treatment and catalysis [58, 60].

### **1.8.1 Biodegradable polymers**

High molecular weight compounds and originally classified as to whether synthetic or natural polymer, degraded physiologically either by enzymes or without to produce biocompatible and safe by-products which are else eliminated by the physiological metabolic pathways [61].

Their applications are growing rapidly in various fields especially in drug delivery systems. Synthetic biodegradable polymers which are mostly hydrophobic materials like alpha-hydroxy acids including polylactide (PLA) and poly (D,L-lactide-co-glycolide) (PLGA), polyanhydrides including polycaprolactone (PCL) and others. Natural biodegradable polymers e.g.: chitosan, dextran and others [62]. Synthetic polymers are often preferred for their higher purity and well-enhanced reproducibility [63].

Biodegradable polyesters, particularly polylactide (PLA), polycaprolactone (PCL) and poly (D,L-lactide-co-glycolide) (PLGA) are widely used polyesters by nanoprecipitation method owing to their diversity and synthetic versatility [10]. They are biocompatible, biodegradable and shape-memory polymers (SMPs) approved by US Food and Drug Administration [64-67].

#### **1.8.1.1 Poly (D, L) Lactide (PDLLA)**

PDLLA is a renowned and well-researched polymer, available commercially as amorphous polyester [68]. It has different mechanical

characteristics and degradation rates than its primary components: semi-crystalline L-isomer (PLLA) and less crystalline D-isomer (PDLA) of polylactic acid (PLA) [69, 70], it is known to hydrolyze completely by the cleavage of its backbone ester bonds to water and carbon physiologically, so that it is considered as biocompatible and biodegradable polymer [71].

#### **1.8.1.2 Poly (D,L-lactide-co-glycolide) (PLGA)**

PLGA is a binary twin polymer joining polylactic acid (PLA) with polyglycolic acid (PGA) through ester linkages, PLA are found in equal ratios of D- and L- lactic acid. It is the most famous polymer among other biodegradable polymers due to its potential for sustained drug delivery, convenient degradation characteristics and tuning the whole physical properties of the polymer-drug template [71, 72]. It can be used as a drug vehicle for different drugs, proteins and other macromolecules and also as a scaffold for tissue engineering [73].

#### **1.8.1.3 Polycaprolactone (PCL)**

PCL is an aliphatic polyester of hexanoate repeated units, it is a substantially hydrophobic, semicrystalline and easily manufactured synthetic polymer [61]. Since its low melting point, exceptional rheological and viscoelastic properties, high drug permeability and long-term degradation, it can be employed into a large range of three- dimensional platforms especially in drug delivery devices, implants and various biomedical applications [74, 75].



One of the most outcoming obstacles of the long-term circulation of NPs is the rapid clearance by reticuloendothelial system (RES) as it labels them as foreign compounds. PNPs are distinctive in that their surfaces can be modified with whether polyethylene glycol (PEG), polyethylene oxide, polysorbate or poloxamine and mostly with PEG since PEGylated NPs which are often known as “stealth” NPs have the potential to increase the bioavailability and reduce the recognition of immune system and consequently prevent opsonization [76, 77]. According to which polymer and method are used, different PNPs in hydrodynamic size, size distribution, charge and morphology could be obtained [78].

### **1.9 Polymeric nanoparticles preparation methods**

Formulation of particulate systems is based into two categories: the first based on the usage of preformed polymers and the second relied on polymerization of monomers. Six methods primarily used for the first which are: nanoprecipitation, emulsion coacervation, salting-out, spray drying, dialysis, emulsion solvent diffusion and solvent evaporation. The second basically included whether emulsion or interfacial polymerization [10].

Encapsulation is considered a smart delivery approach for different drugs especially for drugs with poorly soluble classification as it would decrease the mucosal contact with NSAIDs, mask the unpleasant taste and odor of drugs and enhance therapeutic efficacy compared to conventional drug delivery [10, 79]. Recently, controlled release nanocarriers are burgeoning

to blue sky areas by limitless research in advanced drug delivery systems [80, 81]. The use of them has increased exponentially and gained remarkable attention in the past two decades due to their numerous ranges of biomedical applications. The majority of these nanocarriers used clinically are liposomes and polymer-based nanoparticles [10, 82].

### **1.9.1 Nanoprecipitation**

One of the most employed, scalable, reproducible and rapid method for the encapsulation of drugs and developing polymeric nanoparticles is nanoprecipitation which is also known as solvent displacement method [83], developed by Fessi and his co-workers [84]. Its usage percentage from the all polymer-based encapsulation methods is around 50% [10].

Briefly as described in **Figure 1.4**, this method involves two phases that are miscible to each other, the first in which both the drug and polymer has to be dissolved (solvent phase) and the second could be a mixture of non-solvents which may contain surfactants, typically it is water (non-solvent phase) [83]. After drop-wise addition of organic (solvent) phase to a moderately stirred aqueous phase, a particulate suspension (nanoparticles) is produced.

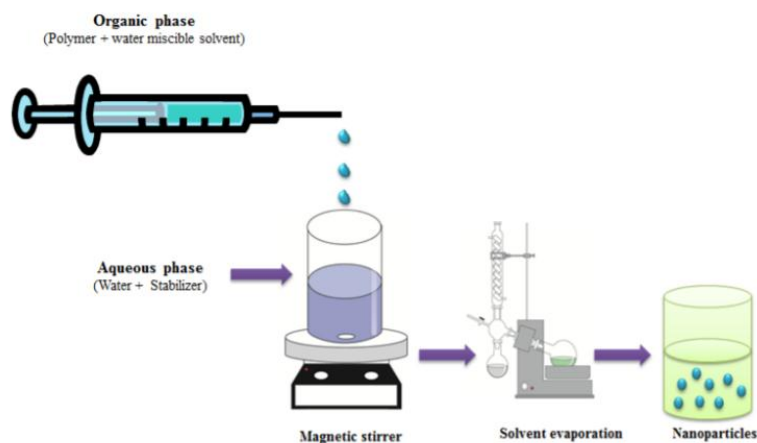


**Figure 1.4:** Nanoprecipitation method [10].

Despite its ease and spread, its low efficiency for encapsulating water soluble drugs, the effect of solvent and amount of polymer used and accordingly controlling particle size distribution restricted its applications [85, 86].

### 1.10 Nanoemulsion

Recently, lipid-based formulations are considered useful choice for delivering drugs and bioactive food components especially those with low oral bioavailabilities and high first-pass metabolism [87]. Nanoemulsion is one of the most commonly used lipid-based nanocarriers as it enhances the solubility and bioavailability of lipophilic drugs [88, 89]. It is a colloidal dispersed system of two immiscible liquids, it is normally oil-in-water (o/w) or water-in-oil (w/o) system that is thermodynamically unstable [90]. It has a size often ranges between 10 to 200 nm [91, 92].

Due to their capability of encapsulating lipophilic components, masking unpleasant taste, simplicity of manufacturing, small droplet size, high

encapsulation efficiency and formulation stability, it attains great interest and fits as a vehicle for the delivery of different pharmaceutical ingredients [90, 93-95].

### **1.10.1 High energy methods**

Nano emulsion drug delivery systems can be formulated using different techniques which are categorized as high energy and low energy methods [96]. High energy methods are widely used to formulate NE by breaking up large droplets to Nano sized particles with high kinetic energy [97, 98]. This method often provides strong disruptive forces, so that greater stability, rheology, and control of the size of particles can be achieved [88, 99]. It comprises: high-pressure homogenization, micro fluidization and ultra-sonication [96].

#### **1.10.1.1 Ultrasonication**

In relation to operation and cleaning, ultra sonication is considered the best of these [100]; it breaks the macro emulsion to Nano emulsion by providing cavitation forces resulting from ultrasonic waves as shown in **Figure 1.5**. The favorable particle size and stability accordingly can be achieved by modifying ultrasonic energy input, intensity and time [101]. It has been largely used for producing nanoemulsions as it produced small-sized droplets with better stability and required less energy input in comparable to the other high-energy methods [102, 103].

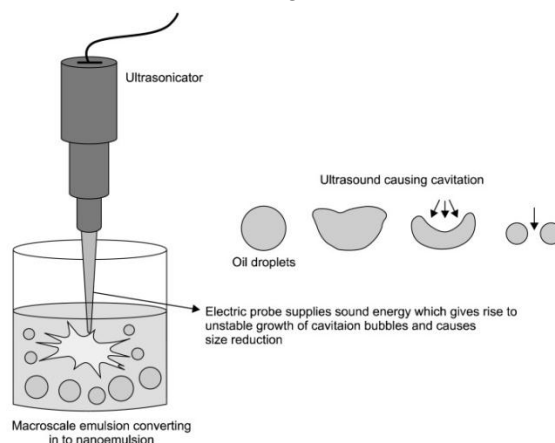


**Figure 1.5:** Ultra sonication technique [104].

## 1.11 Literature review

Encapsulation of NSAIDs gains much of interest recently, as it is considered a smart delivery window for various drugs. It improves the safety, efficacy and overcomes many obstacles regarding them especially using polymeric and lipid-based nanoparticles.

Recently, the preparation of carvedilol-loaded PLA nanoparticles exhibited higher water solubility and sustained release behavior [105]. Moreover, a twin drug of dexamethasone-diclofenac loaded polylactide prepared and showed a sustained release profile with a superior anti-inflammatory activity by Assali et al. [106].

Different nanocarriers were used for encapsulation IND, they were parentally formulated as nanocapsules (NC) for the treatment of Alzheimer disease and inflammation [107, 108], also as polymeric micelle for rheumatoid arthritis using PCL conjugated with  $\beta$ -cyclodextrin and polyethylene glycol (PEG) and this formulation showed increase in the

anti-inflammatory and decrease the side effect. Moreover, a sustained release behavior of IND from this NP [109].

IND was also given topically using different nanoparticles with different composition which all of these shown decreasing the inflammation and increasing skin permeation [110, 111], a sustained release of IND from a liposome [112] in addition to IND loaded into PCL NPs to decrease its side effects and administration frequency. Moreover, an eye drop was prepared using zirconia beads and bead smash 12, this NP formulation showed increasing in the ocular bioavailability and decreasing in the inflammation [113].

A solid NP, Folate-PEG-PAMAM dendrimer and monophasic liposome for IND was formulated orally appeared to increase the bioavailability, decrease the GI side effects, increase uptake into the inflamed joints and decrease intestinal ulceration respectively [114-116].

Different NSAIDs were encapsulated into various PNPs using nanoprecipitation technique, naproxen was encapsulated into different Eudragit<sup>®</sup> formulated into nanocapsules resulting in development of argan oil based nanocapsules with particle size ranges from 100-500 nm for transdermal application [117], also dextran (water-soluble biopolymer) was conjugated with ibuprofen and naproxen by in situ activation of COOH groups using CDI, the resulting derivatives showed high loading efficiency through nanoprecipitation and also the NPs showed good stability over one month on pH ranging from 4 to 11 [118].

A comparative study of diclofenac loaded into PCL nanocapsules prepared by nanoprecipitation and emulsification-diffusion method by Elaissari et al., the results revealed that the smallest particle size and the largest zeta potential were obtained using nanoprecipitation [119]. In addition to *in vivo* studies using both chronic and acute inflammation models of topical formulations of nimesulide-loaded PCL NCS by Lenz and his co-workers. The results showed increasing of anti-inflammatory activities of nanoformulations in comparison to nanocapsules containing free nimesulide [120].

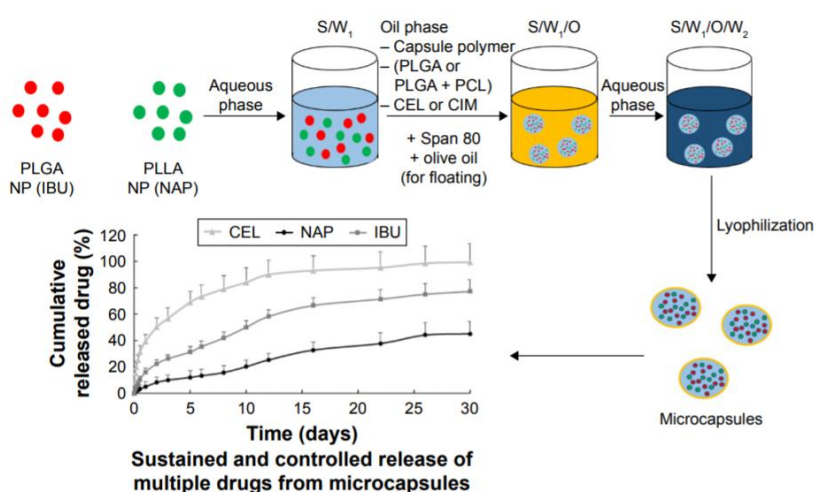
IND was loaded into different PNPs using nanoprecipitation technique; it was loaded into PCL NPs by Badri et al. They developed NC based on argan oil with particle size of 290-350 nm and higher zeta potential values of -40-50 mV [121]. PCL based NPs containing IND has recently been prepared by Elaissari et al., this topical nanoformulation potentiated IND penetration through the skin and decreased the unwanted side effects of it [122]. Furthermore, IND was encapsulated by magnetic PLA NPs and the prepared formulation had a particle size of 250 nm by Závřšová and his co-workers [123].

Various NEs with different compositions were prepared, Howida and co-workers focused on a transdermal alcohol gel and the results showed a prolonged systemic effect up to 32 h for a transdermal IND [124], also a transdermal IND in a combination with sodium hyaluronate (HNa) for enhanced antiarthritic activity by Lassoued et al., HNa-IND NE showed

better antioxidant and skin penetration and an o/w NE loaded with IND presented significant anti-inflammatory than the drug alone as well [125].

A comparison study between IND NEs formed by ultrasonication and spontaneous emulsification by Estelrich and co-workers, the results showed that the low energy method (spontaneous method) had a great stability as its size and polydispersity did not change over more than 2 months [126].

Recently, Loo et al., aimed to resolve the obstacles of chronically using NSAIDs by developing a multi-drug nanosystem using three different NSAIDs which are: ibuprofen, naproxen and celecoxib and adding cimetidine as antacid, encapsulating these into different polymers (PLLA, PLGA and PCL) and then co-encapsulating all of them in a microcapsule as represented in **Scheme 1**. The results revealed an immediate release of cimetidine and a sustained release for the NSAIDs [52].



**Scheme 1:** Schematic representation of the encapsulation of NSAIDs into controlled-release microcapsules [52].



From this literature review, there was no combination between these three drugs IND, PAR and FAM in the literature. Moreover, there is no nanocarriers encapsulates these compounds together and it was the first encapsulation of a well-characterized NE into different polymeric nanocarriers.

### **Aim of the study**

Herein, we intended to synthesize a novel Co-drug of IND and PAR as this would decrease the dose of the parent drugs and intensify their effects, encapsulation of this co-drug into a well-characterized nanoemulsion and the latter into different polymeric nanocarriers using nanoprecipitation technique. These multi component delivery systems, therefore synergize drugs of different mechanisms, remove the obstacles of NSAIDs and allow for sustained release behavior and decrease the GI side effects by adding anti-ulcer drug which is Famotidine.

In addition to characterization of these nanosystems using different analytical techniques: Transmission Electron Microscope (TEM), UV-Vis spectroscopies and Dynamic Light Scattering (DLS). A validated, simple and precise RP-HPLC was developed for determination and quantification of these four different chemical compounds for the first time: IND, PAR, FAM and Co-drug for the *in-vitro* release studies.

## **Objectives**

1. Synthesize the Co-drug of Indomethacin and Paracetamol.
2. Design and encapsulation of Co-drug and Famotidine in the most suitable polymeric nanoparticles system.
3. Characterize the developed multi-component nanosystems using different analytical techniques such as: Transmission Electron Microscope (TEM), UV-Vis spectroscopies, Dynamic Light Scattering (DLS) and zeta potential analysis.
4. Develop and validate a RP-HPLC analytical method.
5. Study the loading, stability and release profiles of the Co-drug and FAM.
6. Study drug release kinetic of Co-drug and FAM from the prepared nanosystems
7. Assess cell biocompatibility of the formed nanosystems.

## Chapter Two

### Reagents and methodology

#### 2.1 Reagents and materials

##### 2.1.1 Co-drug synthesis reagents:

All materials and reagents used with the highest grade of purity. Indomethacin (IND) (Cat. #: 17378), Famotidine (FAM) (Cat. # RHR1055), 4-(Dimethylamino) pyridine (DMAP) (Cat. #: 1122583), N-(3-Dimethylaminopropyl)-N'-ethylcarbodiimide hydrochloride (EDC) 98% (Cat. #: 1892575) were attained from Sigma-Aldrich Co., USA. Paracetamol (PAR) was donated from Sun Pharma Ltd. (Nablus, Palestine).

The product was purified into column chromatography by using silica gel (pore size 60 Å, 40-63 µm particle size, 230-400 mesh particle size, Sigma Aldrich Co.). Thin layer chromatography (TLC) (DC-Fertigfolien Alugram<sup>®</sup> Sil 6 G/UV 254, Macherey Nagel Company, Germany) was used to examine the reaction. A sensitive weighing balance (Adventurer<sup>®</sup>, Ohaus Corporation, USA), water bath sonicator (Elmasonic S 70 Hz, Elma, Germany) and rotary evaporator (Stuart<sup>®</sup> RE400/MS, UK) were also used.

##### 2.1.2 Analysis reagents and chemicals:

Sodium acetate trihydrate, ethyl acetate 99.5% (EtOAc), hexane (Hex) and dichloromethane (DCM) were purchased from CS Co. and acetonitrile supragradient grade for chromatography (ACN) and triethylamine LR (Cat.

#: 40502L05) were purchased from SDFCL. Formulation components: magnesium stearate, microcrystalline cellulose (MCC), croscarmellose sodium (acdisol) and aerosol were awarded from Jepharm Pharmaceuticals Company, Palestine.

### **2.1.3 Nanoemulsions and polymeric nanoparticles preparations reagents:**

Poly (D,L-lactide-co-glycolide) (PLGA) polymer that is an acid terminated with average molecular weight (24,000-38,000) (Cat. #: 71987-0), polycaprolactone (PCL) with average MW 14,000 (Cat. #: 44072-250), D-limonene (Cat. #: 62122-250) were purchased from Sigma-Aldrich Co. Polyoxyethylene cetyl ether (POE) and polyvinyl alcohol (PVA) were purchased from CS Co., New Zealand. Sorbitan monooleate (Span<sup>®</sup>80) (Cat. #: L12099) was purchased from Alfa Aesar, UK. Polyoxyethylenesorbitan monooleate (Tween<sup>®</sup>80) (Cat. #: 278630025) was purchased from Arcos organics, USA. Acetone, methanol (MeOH), dichloromethane (DCM), and isopropyl alcohol were purchased from C.S. Company, Haifa.

### **2.1.4 Release and stability studies reagents:**

Disodium hydrogen phosphate (Cat. #: 7558794), potassium hydrogen phosphate (Cat. #: 7778770), sodium carbonate and sodium bicarbonate were purchased from CS Co., Haifa. Spectra/Por<sup>®</sup> 4 dialysis membranes (12-14 KD molecular weight cutted-off (MWCO), 25 mm flat width, 100

feet length) were gained from Spectrum Laboratories, Inc. esterase enzyme from Porcine liver (PLE) was attained from Sigma Co., USA.

### **2.1.5 Biology tests reagents:**

Dulbecco's free  $\text{Ca}^{+2}$ - Phosphate Buffer Saline (PBS) (REF # 02-023-1A) and L-glutamine solution (REF # 03-020-1B), Pen-Strep Solution (Cat. # 030311B) were attained from biological industries, Jerusalem. RPMI (Cat. # 05669) was purchased from Manassas VA, USA, Trypsin-EDTA solution 1X (Cat. # 59417C), fetal Bovin Serum (Cat. # C8065) and trypan blue solution (Cat. # RNBD6249), MTS (Cat. # G3581) were purchased from Promega, USA.

## **2.2 Instrumentations**

- **Dynamic Light Scattering (DLS):** was applied for size and polydispersity (PDI) measurements obtained at angle of scattering 90 degree and at a temperature of 25°C (280173 Brookhaven Instruments, USA)
- **Zeta potential** was conducted in NanoBrook Omni (Brookhaven Instruments, USA).
- **HPLC** (Waters 1525, Singapore) binary HPLC pump and waters 2298 photodiode Array Detector was used to quantify drugs.
- **Nuclear Magnetic resonance (NMR) spectra:** was recorded on Bruker 500 MHz –Avance III, Switzerland.

- **High-resolution mass spectra data (HRMS):** chemical shifts were measured and coupling constants were conducted in (ppm and hertz (Hz.) respectively.
- **Transition electron microscope (TEM)** images were conducted at 60 kV by using Morgagni 286 transmission microscope (FEI Co., Eindhoven, Netherlands).
- **Esco celculture CO<sub>2</sub> incubator:** for incubating the cell line.
- **Unilab microplate reader 6000:** was utilized in the cell viability test to read the plate.
- **Magnetic stirrers** (Heidolph instruments 20021884 0319, Germany): were used for release studies and preparation of PNPs and NE.

### 2.3 Preparation of the buffers

- **Phosphate Buffered Saline pH 7.4 (PBS)**

One liter stock solution was prepared by adding (0.19, 8 and 2.38 g) of potassium dihydrogen phosphate (PDP), sodium chloride (NaCl) and disodium hydrogen phosphate (DHP) respectively, then dissolved and diluted with distilled water up to 1 liter. Finally, this stock was adjusted with little drops of 1 M HCl [127].

- **Carbonate buffer solution pH 9.2**

1.0599 g anhydrous  $\text{Na}_2\text{CO}_3$  was dissolved and diluted in distilled water up to 100 mL to attain sodium carbonate solution ( $\text{Na}_2\text{CO}_3$ ) with 0.1 M concentration, also sodium bicarbonate ( $\text{NaHCO}_3$ ) with 0.1 M concentration was obtained via dissolving 0.84 g  $\text{NaHCO}_3$  with distilled water and then diluting up to 100 mL vol. flask. After that, 90 mL from 0.1 M  $\text{Na}_2\text{CO}_3$  was supplemented to 10 mL from 0.1 M  $\text{NaHCO}_3$  solution into a 100 mL vol. flask [127].

- **Acetate buffer solution pH 4.5**

From acetic acid with 2 molar conc., 14 mL was put to 2.99 g of Na-acetate, then dissolved and diluted with distilled water up to one liter [127].

## **2.4 Methodology**

All synthetic, analytical and formulated procedures were performed at Pharmacy College Labs (An-Najah National University, Nablus) except for NMR and TEM images were done at University of Jordan and HRMS at Anadolu University, Turkey.

### **2.4.1 Synthesis and characterization of IND-PAR Co-drug:**

8 mL of dichloromethane was put on a mixture of IND (200 mg, 0.60 mmol), PAR (101.4 mg, 0.67 mmol), EDC (128.6 mg, 0.67 mmol) and DMAP (75.1 mg, 0.62 mmole) and was stirred at room temperature (RT) for 24 h. The reaction was treated with DCM and 1M HCl (x3). The

collected organic layers were evaporated using rotary evaporator and the remaining crude was purified by flash chromatography on silica gel eluting with (Hex: EtOAc 1:2) to give a yellowish white solid product with a yield 70% (220 mg) and  $R_f = 0.63$  (Hex: EtOAc 1:2).  $^1\text{H}$  NMR (500 MHz,  $\text{CDCl}_3$ ):  $\delta$  2.11 (s, 3H,  $\text{COCH}_3$ ), 2.42 (s, 3H,  $\text{CH}_3$  indole), 3.81 (s, 3H,  $\text{OCH}_3$ ), 3.86 (s, 2H,  $\text{CH}_2\text{CO}$ ), 6.68 (dd, 1H,  $J = 9.2$  Hz,  $J = 2.3$  Hz, H-7 indole), 6.68 (d, 1H,  $J = 9.2$  Hz, H-9 indole), 6.98 (d, 2H,  $J = 8.8$  Hz, phenyl), 7.02 (d, 1H,  $J = 2.3$  Hz, H-6 indole), 7.45 (dd, 4H,  $J = 8.8$  Hz,  $J = 1.9$  Hz, phenyl), 7.65 (d, 2H,  $J = 8.4$  Hz, phenyl). HRMS (ESI,  $m/z$ ): calcd. for  $\text{C}_{27}\text{H}_{24}\text{N}_2\text{O}_5\text{Cl}$   $[\text{M} + \text{H}]^+$  491.1374, found 491.1372.

#### 2.4.2 Preparation of nanoemulsions

The method was developed in other master thesis project using ultrasonication method [128]. In brief, the organic phase consists of 140 mg of sorbitan monolaurate and 750 mg of D-limonene (Organic phase) weighted into a beaker and sonicated for 5 mins then added dropwise under mild stirring to the aqueous phase that consists of 360 mg of tween 80 and 8.75 mL of milli-Q water. The resultant flocculated emulsion was mildly stirred for 15 min and after that sonicated for 10 min. After preparing and characterizing this blank NE, 2 mg co-drug was loaded into the organic phase of that NE. Finally, the effective diameter, polydispersity index (PDI) and  $\zeta$ -potential were taken. These measurements were taken at  $25^\circ\text{C}$  using angle of scattering as 90 degree (right angel) for the size and PDI. To measure the  $\zeta$ -potential, NE were diluted three times and added to



capillary cells and measured using phase analysis light scattering (PALS) technique.

#### **2.4.4 Preparation of polymeric nanoparticles**

First of all, blank polymeric nanoparticles of PLGA and PCL were prepared applying nanoprecipitation method formerly described and published in our research group [105, 106]. Briefly, the organic phase including 25 mg of each polymer and 5 mg Polyoxyethylene cetyl ether were dissolved in 5 mL solvent (acetone) and supplemented drop by drop to (PVA and milli-Q water) prepared mixture (aq. phase) which consists of 3 g of 1% and 7 g of each respectively through gentle stirring for 30 min till reaching milky suspension. Then, by a rotary evaporator, acetone was evaporated. After that, the formed nanoparticle solution was filtrated via a syringe filter 0.45 to equiform the particle size. Precipitation of these NPs throughout centrifugation for 10 min at 15000 rpm, and then to exclude the remaining PVA, they were washed out with milli-Q water (x3), dissolved next into eppendorfs containing 2 mL milli-Q water and stored at cool place. Finally, size, PDI and  $\zeta$ -potential for each polymer were determined using DLS.

#### **2.4.5 Encapsulating Co-NE into FAM-PNPs**

Using nanoprecipitation technique, the organic phase was prepared by adding 1 mL of the well-characterized Co-NE, 25 mg of the polymer (PLGA or PCL) and 5 mg of POE and 2 mg FAM dissolved in 5 mL acetone. This mixture sonicated for 5 min and then added drop-wisely to

the aq. phase which composed of 3g of 1% and 7 g of PVA and milli-Q water respectively. This mix. was gently stirring for 30 min and then continued the same as mentioned before in preparation of blank polymeric NPs. These two nanosystems also characterized using the dynamic light scattering techniques and TEM images to confirm the loading. The percentage encapsulation efficiency (EE) for FAM and Co-drug were calculated using the next equation.

$$\text{EE (\%)} = (\text{wt. of (FAM/ Co-drug) loaded in nanoparticles}) / (\text{wt. of (FAM/ Co-drug) initially used}) \times 100$$

#### **2.4.6 HPLC analytical method development**

This development was stand on the USP analytical method of Famotidine, Indomethacin and Paracetamol and this study was recently being published [129].

##### **2.4.6.1 Preparation of solutions:**

**Buffer solution pH 6:** It was prepared by dissolving 13.6 g of sodium acetate trihydrate in 750 mL HPLC water, and then 1 mL triethylamine was added, diluted with HPLC water to 1 L and adjusted to pH 6.0 with glacial acetic acid. Mobile phase was firstly prepared using a mixture of Buffer:ACN, 93:7.

**Diluent 1:** The diluent was prepared by dissolving 6.8 g of potassium dihydrogen phosphate (PDP) in 1 L HPLC water and adjusted to a pH 6.0 by glacial acetic acid.

**FAM, IND, PAR and Co-drug standard solutions:** 2.5 mg of each drug was weighed into 25 mL vol. flask; 5 mL methanol was added and then diluted up to 25 mL by diluent 1.

**Standard solution Mixture:** 2.5 mg of each FAM, IND, PAR and Co-drug were diluted with HPLC ACN up to 25 mL.

### **pH, mobile ratio and diluents used in method development trials**

Various mobile phase compositions, pHs and diluents were tested during the analytical method development. The used mobile phases and diluents at different pHs are briefed in **Table 1**.

**Table 1: Brief of method development optimization.**

Drug	Mobile phase		pH	Diluent used
	Buffer	ACN		
FAM and IND mix.	93	7	6	Diluent 1
	93	7	5	
	50	50	5.5	
	60	40	5.5 & 6	
	40	60	5.5 & 5	
Co-drug	40	60	5	Diluent 1
PAR	40	60	5	Diluent 1
				Methanol
				ACN
FAM, Co-drug and IND individually	40	60	5	ACN
Mix. of all drugs	40	60	5	ACN

#### **2.4.6.2 Analytical method validation:**

It was developed accordant with FDA and ICH guidelines and validated using the following parameters: linearity, range, accuracy, precision, robustness, and ruggedness [130]. All parameters were obtained in triplicates.

#### **2.4.6.2.1 Linearity and range:**

It was conducted by preparing a serial five conc. in the range of 0.01 to 0.1 mg/mL from a pre-prepared stock solution of 1 mg/mL. The calibration curves were built by plotting the mean area under the curve (AUC) obtained from the HPLC against conc. The regression equations and the square correlation coefficient ( $R^2$ ) were calculated for each drug curve.

#### **2.4.6.2.2 Accuracy and selectivity:**

Accuracy and selectivity validation parameters were calculated by preparing a standard solution of a mix. of four drugs with a concentration of 0.24 mg/mL for each drug. Three concentration levels of 80%, 100%, and 120% of the standard concentration were prepared. The three solutions were prepared having different excipients: microcrystalline cellulose, magnesium stearate, aerosil, and acidisol. The accuracy was estimated by determining the percentage of recovery. The selectivity of the developed method was examined as the eluted peaks are well separated and not impacted with four aforementioned excipients.

#### **2.4.6.3 Precision:**

It was conducted at three levels. Firstly, instrument precision was made by injecting the standard mixture 9 times; the %RSD of the generated peaks of the chromatogram was calculated. An intermediate precision involving interday and between analyst precision was examined on conc. (0.08 and 0.1) mg/mL respectively. The %RSD was calculated for both mix.

#### 2.4.6.4 Robustness:

It was implemented through conducting negligible changes on method parameters which were mentioned in **Table 2**, these modifications were done by varying mobile phase conditions [131].

**Table 2: Robustness parameters and conditions checked.**

Robustness parameter	Condition examined
pH	4.9, 5.0 & 5.1
Wavelength detected (nm)	270, 275 & 280
Flow rate (mL/min)	1.2 & 1.4

#### 2.3.6.5 Limit of Detection and quantification (LOD & LOQ)

These two detection limits are used as an indicator of the sensitivity parameter. Calculating these two parameters was done by utilizing signal to noise ratio (S/N) in HPLC baseline. LOD & LOQ values of the tested compounds were resolved while the (S/N) is 3 to 1 and 10 to 1 respectively.

#### 2.3.6.3 Statistical analysis

It was conducted on the aforementioned robustness parameters applying the ANOVA test; when the p-value was lower than 0.05, a significant difference was statistically counted. Robustness parameters conducted in triplicates. Statistical results were indicated by means  $\pm$  RSD.

### **2.4.7 In vitro release studies**

#### ***In vitro* release Co-drug and FAM from the whole nanosystems without PLE**

First of all, 10 mg of freeze dried samples from both Co-NE@PCL and Co-NE@PLGA nanoparticles were dissolved into about 3 ml recent preserved phosphate buffer saline (BPS) pH 7.4, then moved out into a dialysis bag (donor compartment). This bag was firmly closed, then with its contents was inserted into 40 mL of PBS at pH 7.4 (acceptor compartment), fully immersed and mildly stirred for more than 3 days at 37°C. Aliquots of 1 mL from each receptor compartment were taken and replaced directly with 1 mL PBS pH 7.4 at determined time periods. These samples were analyzed using HPLC and % release of Co-drug and FAM were calculated along the time.

#### **2.4.7.2 In vitro hydrolysis of Co-drug, Co-drug in nanoemulsion and Co-drug in NE@PNPs**

The synthesized Co-drug was exposed to esterase enzyme to be hydrolyzed to its twins (Indomethacin and Paracetamol). It was done by incubating 1 mg of Co-drug within 10 mL PBS containing 2 mg of PLE at 37°C for 1 h. This method was also applied for hydrolysis of Co-drug into NE, PLGA and PCL nanosystems by adding 1 mL of each of them into the same aforementioned media and mildly stirred for 5 h. Aliquots of 1 mL were attained and substituted with equal volumes of fresh BPS at different time intervals to mimic human body sink conditions, filtered using a syringe

filter (45  $\mu\text{m}$ ) and then analyzed using HPLC. % hydrolysis and % conversion of Co-drug were determined using equations obtained from linearity curves of the developed HPLC validation method.

#### **2.4.8 Drug release kinetics**

To assess the release mechanism for both Co-drug and FAM from the designed and formulated nanosystems, different kinetic models were applied using DDSolver program which helps defining the mechanism of drug release and drug release data and analysis. Comparison between each model and each nanosystem were based on the linear regression ( $R^2_{\text{adjusted}}$ ) [132], the Akaike Information Criterion (AIC) [133], and the Model Selection Criterion (MSC). Data analysis was carried on using the Excel add-in DDSolver program and the best fitted models were taken based on the higher  $R^2_{\text{adjusted}}$  and the lower AIC and MSC values more than 2.0

#### **2.4.9 Stability studies**

##### **2.4.9.1 Stability studies at different temperature**

Both two nanosystems stored at specified temperatures (4-8, 25 and 50°C), effective diameter and PDI measurements were attained at specified time intervals during approximately a month. Moreover,  $\zeta$ -potential measurements were carried on for the first and the last day of a month.

## **2.4.9.2 Stability studies using different buffers**

### **2.4.9.2.1.3. Stability studies:**

It was determined at two different pHs. Two stocks of each nanosystems obtained by diluting 1.5 mL of each with 1.5 mL of each buffer, aliquots were taken for DLS and  $\zeta$ -potential measurements during 1 month.

## **2.4.10 Cell biocompatibility tests**

### **2.4.10.1 Cell line**

The cytotoxicity of both nanosystems was inspected on HeLa cancer cells and 3T3 fibroblasts.

### **2.4.10.2 Cell culturing**

Both cells were cultured in T-175 cell culture flasks enriched with cell culture growth medium (CGM) consisted of RPMI basal medium supplemented with L-glutamine (1%), fetal bovine serum (FBS) (10%), and penicillin/streptomycin (1%). They were preserved in standard cell culture incubator at specified conditions (5% CO<sub>2</sub>, 37°C and 99% humidity).

Concerning sub-culturing, the medium was suctioned and washed with excess of Ca<sup>2+</sup>-free PBS. After that, the cells were incubated with 0.025% trypsin for up to 5 min in the cell culture incubator until sufficient cells separated from the flask. Then, trypsin was inactivated by CGM, the cell suspension was gathered and the viable cell count was counted using trypan



blue stain before adjusting the cell concentration to 50.000 cell/mL. Finally the cells were seeded in 96-well plate as 5000 cell/well. The cells were left to adhere and accommodate overnight before running any test.

#### **2.4.10.3 Cell biocompatibility test**

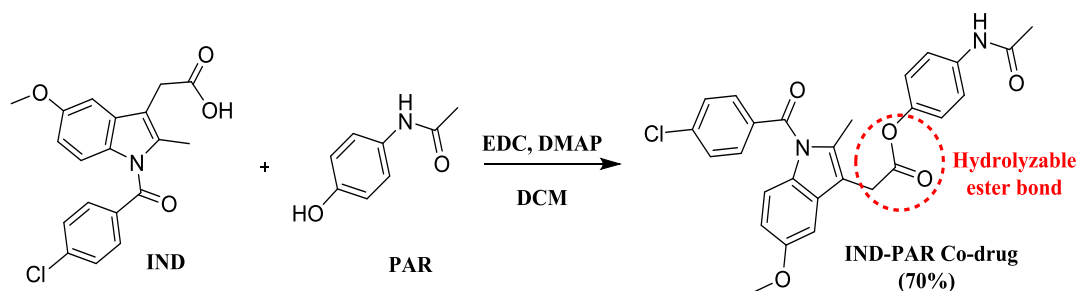
Both normal and cancerous cells were implanted in 96-well plates and then incubated per well with 100  $\mu$ L culture growth media which was supplemented with particular conc. from the tested Co-NE@PCL and Co-NE@PLGA nanoparticles for 24 h. After that, they were incubated with 20  $\mu$ L per well of MTS reagent for 2 h at determined conditions (37°C and 5% CO<sub>2</sub>). Lastly, the abs. of each conc. was determined via a plate reader at specified wavelength 490 nm.

## Chapter three

### Results and Discussion

#### 3.1 Synthesis of IND-PAR Co-drug

Herein, we aim to synthesize a Co-drug of IND and PAR in order to have a superior synergistic analgesic, antipyretic and anti-inflammatory activities. This synthesis was achieved by the formation of an ester bond between joining the parent drugs (IND & PAR), utilizing a carbodiimide reagent which is EDC and acts as a coupling agent and DMAP as a base and this represented in **Scheme 2**. The Co-drug was excellently synthesized for the first time with a high yield of 70% (yellowish white solid product). The Co-drug strategy is often utilized for synergistic effects and enable dose reduction of the parents drugs [134, 135].



**Scheme 2:** Synthetic scheme of Co-drug.

The synthesized (IND-PAR) Co-drug was fully characterized by NMR, HRMS and HPLC with a purity of more than 99%.

### 3.2 Preparation of nanoemulsion

The small size nanoemulsion was obtained by using a couple of nonionic surfactants which were Span 80 and tween 80, they were used because they hold the same backbone, so that they can easily mix together since tweens are polyoxyethylene derivatives of sorbitan fatty acid esters (spans), resulting to a controlled change in the last HLB. The HLB with a range of 9 to 12 is considered the optimum for these two surfactants mixtures [136] and the stability can be enhanced by these two surfactants [137]. This o/w nanoemulsion was prepared by suitable proportions of water, surfactants and oil without the addition of co-surfactants.

Recently, formulating fruit flavor NE is expected to enhance color, particle size, viscosity, solubility and pH as this would increase the acceptance by the consumers [138]. Therefore, D-limonene has been added to this formulation as an oil, it is a main flavor extracted from citrus fruits and widely used as flavoring additives [139]. It has previously been used in preparing NE as it decreased the particle size and enhanced the stability [128]. Herein, we loaded Co-drug into fruit flavor NE because the parent drugs have unpleasant bitter taste and also to mask the disagreeable odor of sorbitan fatty acids [140]. Interestingly, this colorless monocyclic monoterpene promotes gastric ulcer healing by increasing mucus production with no apparent toxic effects and displays anti-inflammatory activity by decreasing different types of protective chemicals as well [141, 142].

The resulting yellowish nanoemulsion was characterized by TEM in order to confirm the formed spherical colloidal structure as represented in **Figure 3.1**. Moreover, the hydrodynamic size and  $\zeta$ -potential of the outcoming NEs were measured. A small nanoparticle size for the formed NE was obtained having a range of 1.5-2.5 nm with highly stable nanoemulsions as the zeta potential data were above 35 mV. It was noticed that the size was slightly increased in the size of the Co-drug loaded nanoemulsion due to the loading of the Co-drug. Moreover, the loading efficacy was 100% of the loaded Co-drug in the NE. Therefore, the formed NE was a small-sized, stable and monodisperse fruit-flavor NE which allowed for greater absorption due to small-sized droplets with greater surface area [93]. These measurements were summarized in **Table 3**.

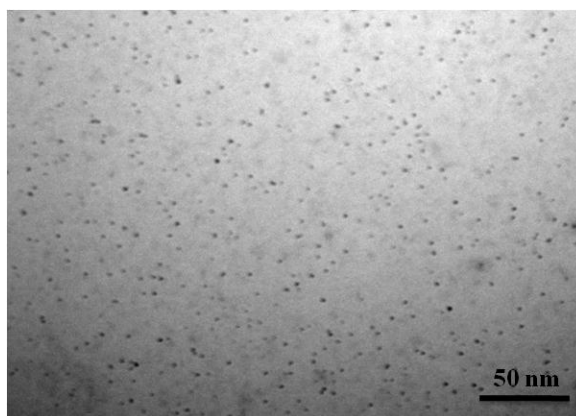


**Figure 3.1:** TEM image showed the morphology of the formed nanoemulsion.

**Table 3: Characterization of blank and Co-NEs.**

Nanoemulsions	D-Limonene (Blank) NE	Co-NE
Hydrodynamic size (nm)	1.64	2.33
Polydispersity index	0.162	0.272
Zeta potential (mV)	-38.02	-47.77

### 3.3 Preparation of polymeric nanoparticles

The particles were prepared using nanoprecipitation and different parameters were controlled until finding the best amount of polymers for both hydrodynamic size and loading capacity which was 25 mg as developed in our research group [105]. In addition, the nanoparticles were decorated with polyethylene oxide which acts as a masking agent against opsonization for the drug transporter and accordingly prevents phagocytosis by mononuclear phagocyte system (MPS) [143]. Moreover, acetone was the best solvent for obtaining the smallest particle size with the narrowest size distribution by decreasing the interfacial tension at first and increasing the removal rate from the particles which resulting in solidifying the particles quickly and finally decreasing the particle size [144].

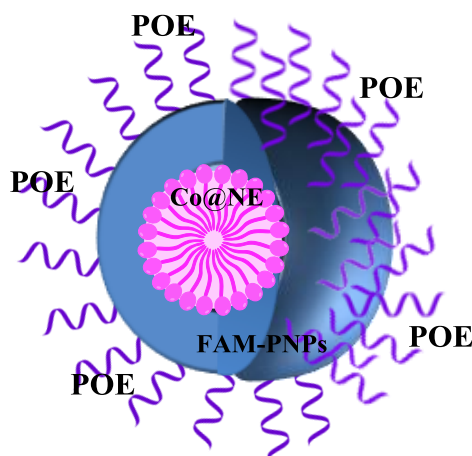
In this study, PLGA and PCL naked nanoparticles have been prepared using 25 mg of each, the results showed good formation of the nanoparticles with acceptable zeta potential results comparing to 12.5 mg and the data were mentioned in **Table 4**.

**Table 4: Characterization of PNPs.**

PNPs	PLGA NPs	PCL NPs
<b>Hydrodynamic size (nm)</b>	219.53	271.00
<b>Polydispersity index</b>	0.138	0.074
<b>Zeta potential (mV)</b>	-26.71	-27.19

### 3.4 Encapsulating Co-NE into FAM-polymeric nanoparticles

After the successful formation of the co-drug loaded in the nanoemulsion, we attend to administer Famotidine with the loaded nanoemulsion in one formula. Therefore, we aim to co load the Co-NE with Famotidine inside two types of polymeric nanoparticles as shown in **Scheme 3**. For that reason, the Co@NE and Famotidine were added to the organic phase upon the preparation of PCL or PLGA nanoparticles.



**Scheme 3:** Schematic representation of the whole nanosystem.

In order to confirm the formation and encapsulation of NE into the PCL or PLGA nanoparticles, the formed nanoparticles were characterized by TEM, DLS and zeta potentials. **Figure 3.2** shows the TEM images of PCL and PLGA nanoparticles loaded with Famotidine and Co-NE as it can be observed the double layers formation of nanoemulsion surrounded the PCL or PLGA nanoparticles.

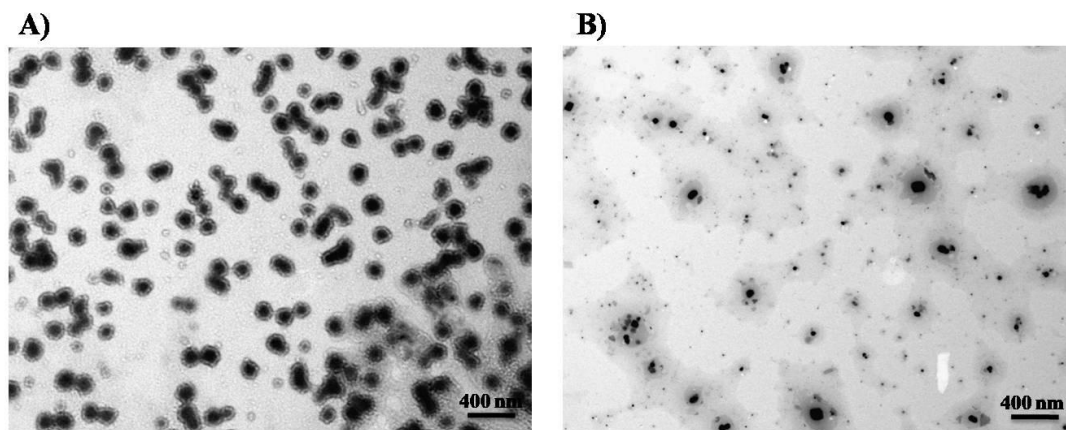


**Figure 3.2:** TEM images for both nanosystems of **A)** Co-NE@PCL and **B)** Co-NE@PLGA nanoparticles.

Both attained multi-component NPs was characterized in addition to TEM, hydrodynamic size, PDI and zeta potential. The results as mentioned in **Table 5** showed that these two nanosystems were with desired size, monodisperse with sufficient stability as zeta potential for both were above -30 mV.

Zeta potential values give an indirect way for measurement of the net charge on the surface of NPs; enhance their physical state in liquids and accordingly their interactions with biological systems. Zeta potential values of  $\pm 20$ -30 considered moderately stable and higher than  $\pm 30$  were considered highly stable NPs [140].

In the interest of determining the encapsulation efficiency, and for the *in vitro* release profiles, a validated HPLC method was developed as shown in the following sections.

**Table 5: Characterization of PLGA and PCL nanosystems.**

Multi-component nanosystems	PLGA nanosystem	PCL nanosystem
Hydrodynamic size (nm)	241.38	196.36
PDI	0.271	0.216
Zeta potential (mV)	-43.04	-39.42

### 3.5 HPLC analytical method development

#### 3.5.1 Method development

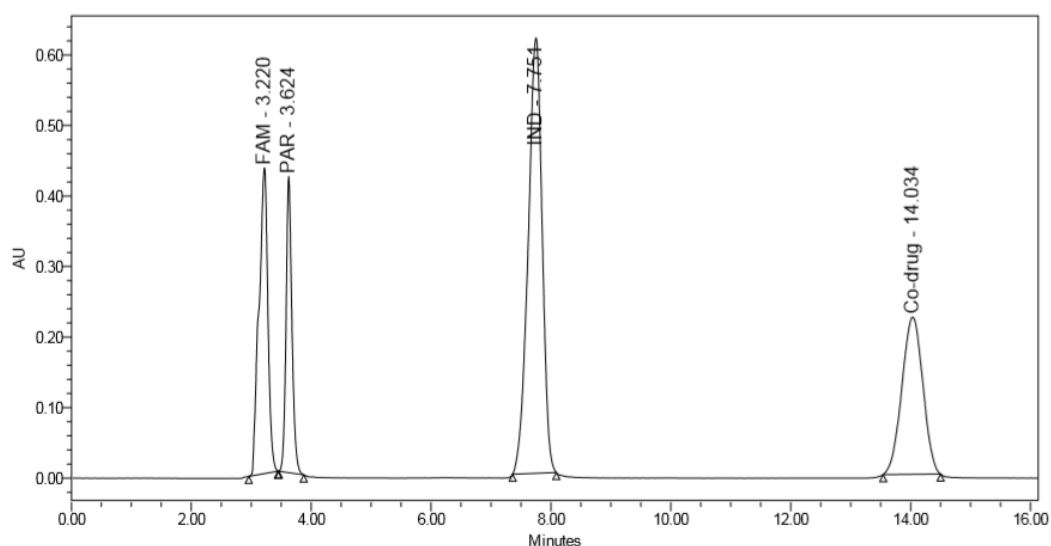
A reverse phase HPLC analytical method was developed and validated accordant with ICH guidelines [145] and recently being published [146] as seen in **Appendix A**. The method was generally relied on the USP analytical method of Famotidine and Indomethacin and was later optimized and validated for getting the optimum separation for the four components.

Several trials were performed to attain the best separation by mainly modifying the pH and the ratios of mobile phase mixture and as well as the diluent used for the component mixture until getting the best well-separated peaks. The ultimate chromatographic specifications for the developed HPLC run are summarized in **Table 6**. The eluted peaks were symmetrical with narrow broadening eluted at different retention times: 3.220, 3.624, 7.751 and 14.034 min. for FAM, PAR, IND and Co-drug respectively as shown in **Figure 3.3**.



**Table 6: The HPLC chromatographic conditions.**

HPLC Chromatographic conditions	
Flow rate	1.4 mL/min
Wavelength ( $\lambda$ )	275 nm
Stationary phase	XTERRA <sup>®</sup> MS C18, 5 $\mu$ m, 4.6 $\times$ 250 mm cartridge
Column T	25 $^{\circ}$ C
Injection V	10 mL
Run time	20 min

**Figure 3.3:** Chromatogram of the eluted peaks for the component mixture.

### 3.5.2 Method validation

#### 3.5.2.1 Linearity and range:

Linearity of the method was measured by plotting the area under the curve obtained from the HPLC of each drug against the corresponding concentrations. The linearity was demonstrated over the concentration

range (0.01-0.1 mg/mL) for FAM, PAR, IND and Co-drug respectively. The goodness-of-fit ( $R^2$ ) was found to be more than 0.99 demonstrating a linear relationship between the conc. of the analytical sample and the noticed peak area. Regression line slopes for FAM, PAR, IND and Co-drug are shown in **Figure 3.4**.

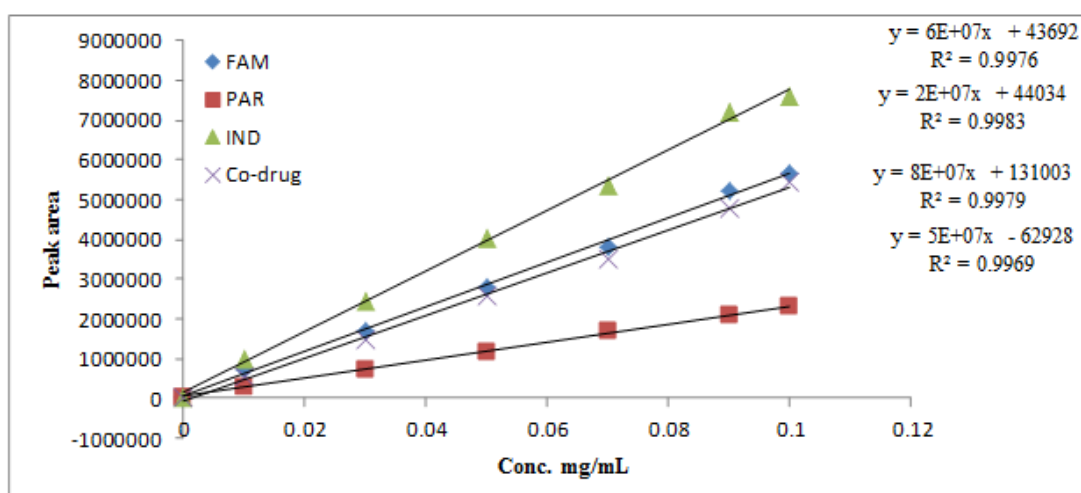


**Figure 3.4:** Linearity curves for the four compounds.

### 3.5.3.2 Accuracy and selectivity:

The four drugs components (FAM, PAR, IND, and Co-drug) were formulated with the following inactive ingredients: microcrystalline cellulose, magnesium stearate, aerosil and acdisol to study the accuracy and selectivity of the developed analytical method [147].

These two parameters were investigated to avoid any interference of the added four excipients which were used for tablet formulation on the separations and peak areas of the measurements ingredient mixture and this was clear from **Figure 3.5**. The peaks were well-separated as no

interference with the inactives and also the elution times for all were not changed.

The method showed great accuracy within the tested concentration range (0.08-0.12). The percentage of the RSD and percentage of recovery for all tested solutions are within the reasonable limits ( $100 \pm 2\%$ ); the collected data is shown in **Table 7**.

**Table 7: The accuracy results in the conc. range (0.08-0.12) mg/mL.**

Conc. (mg/mL)		FAM	PAR	IND	Co-drug
0.08	Av. Area	3070661.67	1868718.67	6561098.33	3306252.67
	%RSD	0.89	1.46	0.97	0.86
	%Recovery	99.34	100.76	100.73	99.5
0.1	Av. Area	4294603.67	2347628.33	7736858.33	4166430.33
	%RSD	0.64	0.67	1.42	0.59
	%Recovery	99.5	99.98	99.22	101.38
0.12	Av. Area	5238679.0	2886956.67	9774300	5300362.67
	%RSD	1.23	1.79	0.36	1.24
	%Recovery	100.33	100.89	100.88	100.82

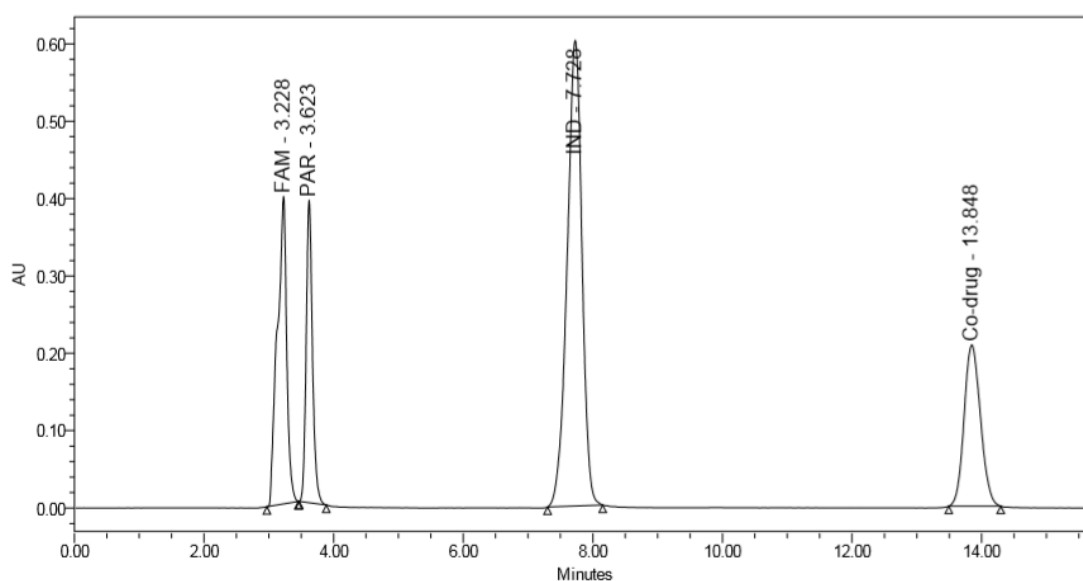


**Figure 3.5:** Chromatogram of the eluted peaks for the component mixture with the inactive ingredients.

### 3.5.3.4 Precision:

This parameter was examined at distinct levels; system precision was tested by syringing 0.1 mg/mL 9 times on HPLC and the %RSD was found to be less than 2.0 for all tested compounds.

Intermediate precision validation parameter at different days (intraday precision) was studied by performing three replicates measurements at two different concentrations (0.08 and 0.1 mg/mL). The results showed that the %RSD of the triplicate of each concentration was less than 2.0. Furthermore, the repeatability was tested for different analyst was by doing three replicates of measurements for the mixture at 0.12 mg/mL and the %RSD results were also less than 2.0. The precision results at different precision levels are demonstrated in **Table 8**.

**Table 8: The precision results at different precision levels.**

<i>Products</i>		<i>FAM</i>	<i>PAR</i>	<i>IND</i>	<i>Co-Drug</i>
<b>System precision</b>	<b>0.1 (mg/mL)</b>				
	<b>Av. Area</b>	4227059	2314677	7742724	4178095
	<b>%RSD</b>	0.80	1.66	1.30	1.64
<b>Intraday precision</b>	<b>0.08 (mg/mL)</b>				
	<b>Av. Area</b>	3147937	1904973	6560894	3288773
	<b>%RSD</b>	1.66	0.70	0.97	1.33
<b>Interday precision</b>	<b>0.1 (mg/mL)</b>				
	<b>Av. Area</b>	4204444	2317970	7736858	4098577
	<b>%RSD</b>	0.76	1.75	1.42	0.20
<b>Different analyst</b>	<b>0.12 (mg/mL)</b>				
	<b>Av. Area</b>	5249199	2878872	9739513	5286421
	<b>%RSD</b>	0.88	0.95	0.49	1.60

### 3.5.3.5 Detection and quantification limit (LOD & LOQ)

The detection limit or LOD is the lowest amount of analyte in a sample that can be detected. It may be expressed as a concentration that gives a signal-to-noise ratio of approximately 3:1. While the limit of quantification or LOQ is the lowest amount of analyte in a sample that can be determined with acceptable precision and accuracy with a signal-to-noise ratio of approximately 10:1 can be taken as LOQ. The LOD was calculated for FAM, PAR, IND and Co-drug. It was found to be  $3.076 \times 10^{-9}$ ,  $3.868 \times 10^{-10}$ ,  $1.066 \times 10^{-9}$ , and  $4.402 \times 10^{-9}$  mg/mL respectively. While the calculated LOQs were  $9.322 \times 10^{-9}$ ,  $1.172 \times 10^{-10}$ ,  $3.232 \times 10^{-9}$ , and  $1.334 \times 10^{-8}$  mg/mL respectively.

### 3.5.3.6 Robustness:

The robustness of an analytical procedure was tested by measuring its capacity of the developed method to remain unaffected by small but deliberate variations in the method parameters and provides an indication of its reliability during the normal use. For this study the flow rate, wavelength and pH parameters were changed for mixture of 0.1 mg/mL. The results are summarized in **Table 9**. Obviously, the %RSD values in all tested and varied parameters were found to be less than 2.0 which indicate good robustness for the developed method. Besides, the ANOVA test reveals no significant difference for the tested compounds for all robustness validation parameters (p-value > 0.05).

**Table 9: Results of robustness validation parameters.**

		<i>FAM</i>	<i>PAR</i>	<i>IND</i>	<i>Co-drug</i>
<i>The wavelength of maximal absorption (<math>\lambda_{max}</math>)</i>					
<i>273 nm</i>	<b>Av. Area</b>	4279022	2357627	7713100	4191009
<i>275 nm</i>	<b>Av. Area</b>	4225523	2324816	7797471	4109888
<i>277 nm</i>	<b>Av. Area</b>	4263527	2374482	7759887	4186203
	<b>%RSD</b>	0.65	1.07	0.54	1.09
<i>Mobile pH</i>					
<i>pH 5.1</i>	<b>Av. Area</b>	4353746	2280521	7609836	4089088
<i>pH 4.9</i>	<b>Av. Area</b>	4355659	2247925	7803400	4177253
<i>pH 5.0</i>	<b>Av. Area</b>	4225523	2324816	7797471	4109888
	<b>%RSD</b>	1.73	1.69	1.42	1.12
<i>Flow rate</i>					
<i>Flow rate of 1.2 mL/min.</i>	<b>Av. Area</b>	4289108	2336035	7620148	4220573
<i>Flow rate of 1.4 mL/min.</i>	<b>Av. Area</b>	4225523	2324816	7797471	4109888
	<b>%RSD</b>	1.06	0.34	1.63	1.88

**3.5.3.7 System suitability:**

System suitability tests are used to verify that a system is performing adequately to ensure confidence in the analytical method and the results obtained. The developed method showed that all of the standard system suitability parameters including the resolution, symmetry of the peaks and theoretical plates and retention factor (K) are within acceptable limits as displayed in **Figure 3.6**. The data are outlined in **Table 10**.

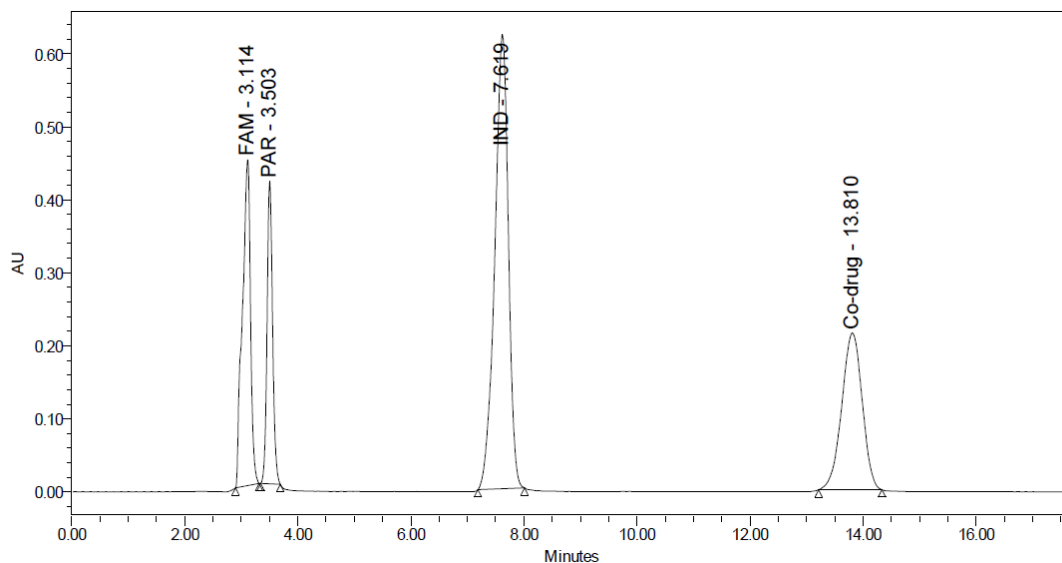


**Figure 3.6:** Chromatogram for system suitability.

**Table 10: System suitability.**

	<i>FAM</i>	<i>PAR</i>	<i>IND</i>	<i>Co-drug</i>
<i>Resolution (R)</i>	1.2	6.8	6.7	7.5
<i>Symmetry of the peaks</i>	1.1	0.9	1.1	1
<i>Theoretical plates (N)</i>	1418	2101	2160	6499
<i>Retention factor (K)</i>	1.67	2.08	5.41	10.42

### 3.6 Encapsulation efficiency (EE)

Herein, the size distribution of NPs was narrow and the encapsulation efficiency for both Co-drug and FAM was high as seen in **Table 11**. It seems higher for Co-drug than FAM, this mainly due to increasing loading capacity with lipophilic drugs in comparable to hydrophilic FAM drug especially when nanoprecipitation method is used [78]. Moreover, Co-drug loaded into lipophilic NP which is nanoemulsion and this considered an additional lipohilicity and NE often provides high encapsulation efficiency especially for lipophilic drugs.

**Table 11: EE values for Co-drug and FAM.**

Nanosystems	<i>PCL nanosystem</i>		<i>PLGA nanosystem</i>	
% EE	<i>Co-drug</i>	<i>FAM</i>	<i>Co-drug</i>	<i>FAM</i>
	100	85	100	70

### 3.7 In vitro release studies

The developed HPLC analytical method was utilized for examining the conversion of Co-drug to Indomethacin and Paracetamol *in vitro*, Co-drug at nanoemulsion (Co-NE), Co-drug in both nanosystems (PCL and PLGA nanosystems) (Co-NE@PNPs) in the existence of PLE enzyme (1 U/mL) in PBS (pH 7.4) 37°C.

#### 3.7.1 % Conversion of Co-drug, Co-NE and Co-NE@PNPs

For the conversion of the Co-drug to Indomethacin and Paracetamol, we used esterase enzyme as the formed ester hydrolysable bond through the incubation with PLE enzyme, a lowering in Co-drug HPLC peak along with gradual increasing of both IND & PAR peaks and this was assessed through the acquired equations from linearity section. As seen in **Figure 3.7 A**, the entire conversion was noticed over an hour with a half-life 12.2 min. For the conversion of Co-drug loaded into NE, it was found that Co-drug HPLC peak was gradually decreased and took a longer time to have more than 80 % conversion which about 5 h as observed in **Figure 3.7 B**. The conversion of Co-drug into PNPs was also investigated upon incubation with esterase enzyme. For Co-drug NE loaded into PLGA. The conversion of Co-drug was gradually increased as Co-drug HPLC peaks



decreased in a slower rate than before; it took about 6 h of co-drug to be 85% converted as seen **Figure 3.7 C**. The same also with PCL PNPs except for constant conversion of Co-drug after 2h and for PLGA after 3 h and that was clear from the **Figure 3.7 D** listed below.

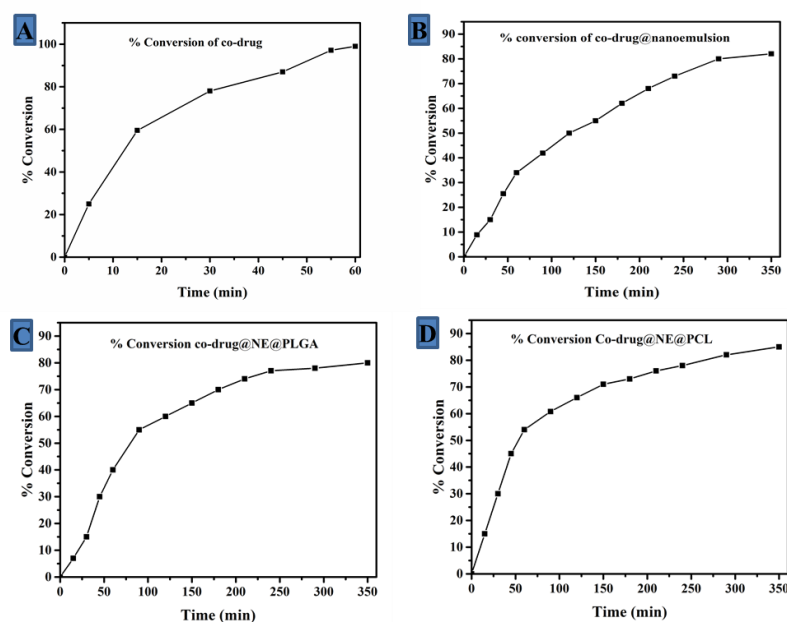


**Figure 3.7:** % Conversion of Co-drug. **A)** % Conversion of free Co-drug, **B)** % Conversion of Co-NE, **C)** % Conversion of Co-NE@PLGA NPs and **D)** % Conversion of Co-NE@PCL NPs.

### 3.7.2 *In vitro* release of Co-drug and FAM without PLE

*In vitro* release profiles of both Co-drug and FAM were investigated using the dialysis membrane. It observed an initial burst of about 10 and 22% of Co-drug from PLGA and PCL nanosystems respectively especially in the first 20 min accompanied by a sustained release of about 80 and 90% for Co-drug from PLGA and PCL nanosystems respectively for more than three days as displayed in **Figure 3.8 A** and **B**.

The release profile of FAM from PLGA nanosystem, it gave an initial burst of about 25% and this increased rapidly during the first 20 min until reaching a steady state of approximately 60% for more than three days. In return to the release of FAM from PCL nanosystem, FAM released in higher amounts from PCL reaching about 40% and followed by a rapid increase of about 80% in the first 10 min and followed by approximately 70% sustained release that occurred within more than 80 h.

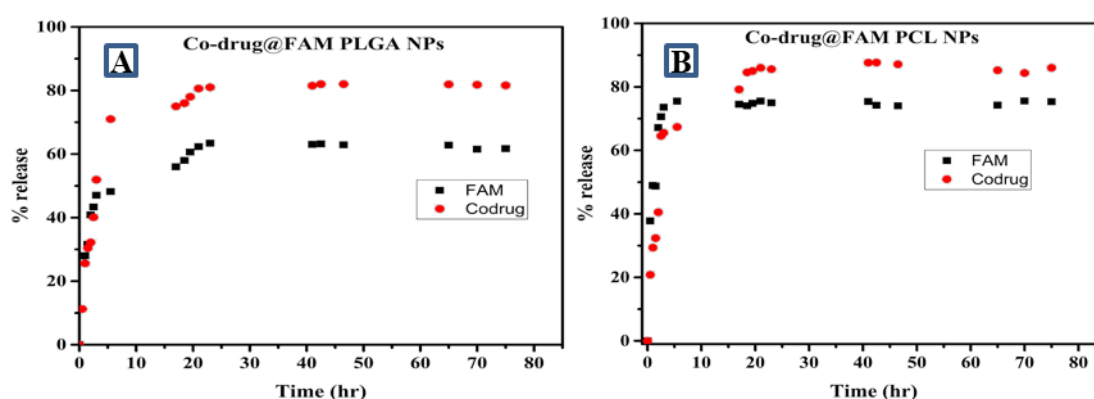


**Figure 3.8:** % Release of Co-drug and FAM. **A)** PLGA nanosystem, **B)** PCL nanosystem.

### 3.8 Drug release kinetics

*In vitro* release profiles were investigated by kinetic modeling. To discriminate the most appropriate model,  $R^2_{\text{adjusted}}$ , the AIC and the MSC were determined [133, 148]. The coefficient of determination ( $R^2$ ) for the best model should be with the higher  $R^2_{\text{adjusted}}$  [132]. For the Akaike Information (AIC) when comparing two models, the lower AIC model would be the better model [149]. MSC is gained more attention in the domain of dissolution data modeling which means the data fits well to the model and a value of more than 2 or 3 of MSC shows a good fit [150, 151].

The results for the curve-fitting studies revealed that FAM release from PLGA nanosystem could be best designed by Makoid-Banakar model whereas first-order with  $F_{\max}$  would be the best for Co-drug as seen below in **Table 12** which showed that  $R^2$  for FAM and co-drug was above 0.97, AIC for these two models were the lowest and MSC were above 2 for both drugs as represented in **Table 12**. Makoid-Banakar is an example of semi-empirical model which represents first-order nearly similar to zero order process [152]. Regarding to other findings, it usually clarify dissolution behavior from controlled release dosage forms [153, 154].

It was noted that the best model of FAM from PCL nanosystem was Weibull which suggested that FAM was released from spherical polymeric matrix with a sustained release manner. Interestingly, Weibull which is known as stretched exponential, is the highly common model applied to outfit diffusion-controlled experimental data [155, 156].

For both nanosystems, the most suitable model for Co-drug was first order with maximum release fraction ( $F_{\max}$ ) values 82% and 85.99% of co-drug from PLGA and PCL nanosystems, where the rate was concentration dependent and these results were in accordant with Co-drug hydrolysis in which first-order kinetic model were the most suitable.

**Table 12: The most fitted models for both nanosystems.**

Nanosystem	Drug	Kinetic model	$R^2_{\text{adjusted}}$	AIC	MSC
PLGA nanosystem	<i>FAM</i>	Makoid-Banakar	0.9790	93.81	3.06
	<i>Co-drug</i>	First-order with $F_{\text{max}}$	0.9887	99.06	4.02
PCL nanosystem	<i>FAM</i>	Weibull	0.9756	100.79	2.51
	<i>Co-drug</i>	First-order with $F_{\text{max}}$	0.9705	116.98	2.98

### 3.9 Stability studies

The stability of both nanosystems was investigated by varying the temperatures (4-8, 25 and 40 °C) and the pH (4.5 and 9.2) as explained in the following sections.

#### 3.9.1 Stability studies at different temperatures

The stability of both nanosystems was tested at different temperatures (4-8, 25 and 50°C). It was studied by analyzing the size of particles and the  $\zeta$ -potential as a function of time. For PCL nanosystems, it was obvious from **Table 13** that this system is more stable than PLGA nanosystems at the three different temperatures as particle size and polydispersity changes are within the acceptable limits and doesn't exceed a size above 240 nm and polydispersity also less than 0.3 for all measurements and that results were with agreement that PCL polymer considered as a long-term stable polymer [75].

For PLGA nanosystems, it was clear that the optimum storage condition was the cold temperature as small changes on particle size and this result was concordant with other research findings [157, 158]. In opposite to room temperature where was found an increase in particle size and

polydispersity index values especially after 20 days and for the highest T, the results showed an increase of the size in the first days followed by slightly changes until month. However, this nanosystem is also considered stable as there is no sudden increase of both particle size and polydispersity measurements. Moreover, zeta potential measurements were taken for the last readings to confirm stability after one month, and the results showed both of them were stable with higher measurement for PCL nanosystem.

**Table 13: Stability study at different Temperatures.**

Multi-component nanosystems	PLGA nanosystem			PCL nanosystem		
	Temperature °C			Temperature °C		
	4-8	25	50	4-8	25	50
Hydrodynamic size (nm) at first day.	119.52	127.47	182.9	189.29	178.03	222.13
Polydispersity index at first day.	0.255	0.247	0.213	0.190	0.176	0.134
Hydrodynamic size (nm) after one month.	117.81	165.44	200.29	229.60	181.19	214.71
Polydispersity after one month.	0.255	0.301	0.195	0.061	0.196	0.181
Zeta potential after one month.	-33.06	-29.17	-29.97	-30.48	-32.31	-33.53

### 3.9.2 Stability studies using different buffers

Both nanosystems stability were also assessed at alkaline and acidic buffer solutions. With regard to PCL nanosystem in acetate and carbonate buffers solution, the particle size and polydispersity index measurements almost were not altered during one month, also the results showed a slightly decrease in both measurements as shown in **Table 14**. Even PCL is biodegradable, it is more stable in contrast to polylactides due to lesser

frequent ester bonds per monomer, and for that reason, PCL degradation and hydrolysis take a longer time to be chemically hydrolyzed [159].

Regarding to PLGA nanosystems, there was a decrease in particle size in acetate buffer in the first days and then this size nearly was not changed with polydispersity less than 0.3. However, the alkaline condition appeared for increasing particle size but polydispersity measurements were within the limits.

**Table 13: Stability studies using acidic and alkaline buffers.**

Multi-component nanosystems	PLGA nanosystem		PCL nanosystem	
	<i>Acetate buffer</i>	<i>Carbonate buffer</i>	<i>Acetate buffer</i>	<i>Carbonate buffer</i>
Hydrodynamic size (nm) at first day.	204.54	218.72	209.38	214.77
Polydispersity index at first day.	0.281	0.292	0.100	0.128
Hydrodynamic size (nm) after one month.	171.45	251.84	206.33	206.07
Polydispersity after one month.	0.283	0.270	0.152	0.187

### 3.10 Cellular biocompatibility test

It is very essential to determine the biocompatibility of both developed nanosystems. For that reason, we have investigated the cellular compatibility on HeLa cells and 3T3 fibroblast cells. The viability test was obtained using MTS assay to ascertain the percentage of viability of the cells upon their incubation with the developed nanosystems after 24 hours. As can be observed in **Figure 3.9**, the both cell lines were incubated with various concentrations (25-400  $\mu\text{g/mL}$ ) of the developed nanosystems. The results showed excellent viability of both cell lines which confirm the

biocompatibility of Co-NE@PCL and Co-NE@PLGA nanoparticles. These preliminary data supports to go further *in vivo* studies in the future.

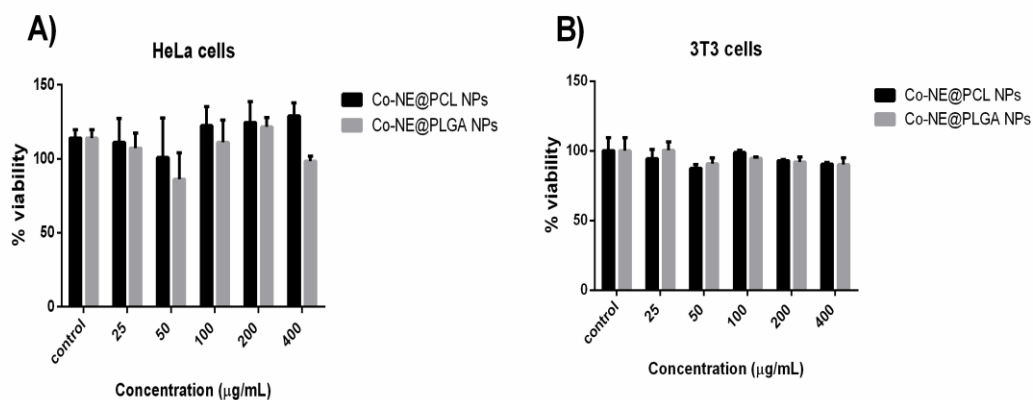


**Figure 3.9:** Viability assay of Co-NE@PCL and Co-NE@PLGA nanoparticles incubated with **A)** HeLa cells; **B)** 3T3 fibroblast.

## Conclusion

In this study, two multi component nanosystems were successfully designed and obtained for effective anti-inflammatory therapy utilizing two different nanocarriers which were nanoemulsions and polymeric nanoparticles. Two encapsulation steps were involved. At first, a synthesized IND-PAR Co-drug was encapsulated into a fruit-flavor nanoemulsion and the second was encapsulation the latter into polymeric nanoparticles having H<sub>2</sub> antagonist drug (Famotidine). These nanosystems were characterized using different techniques and their sustained release manners and hydrolysis of Co-drug were studied by a novel, developed and validated RP-HPLC analytical method. These two nanosystems are biocompatible and had good stability at different conditions. Subsequently, they are promising platforms for overcoming the obstacles of NSAIDs and enhancing patient compliance to their therapy. To best of our knowledge, it was the first study which provides an encapsulation of small-sized nanoemulsion loaded with Co-drug into polymeric nanoparticles having FAM applying nanoprecipitation technique.



## References

1. Laroux, F.S., **Mechanisms of inflammation: the good, the bad and the ugly**. Front Biosci, 2004. **9**: p. 3156-3162.
2. Ricciotti, E. and G.A. FitzGerald, **Prostaglandins and inflammation**. Arteriosclerosis, thrombosis, and vascular biology, 2011. **31**(5): p. 986-1000.
3. Scott, A., et al., What is "*inflammation*"? *Are we ready to move beyond Celsus?* **British journal of sports medicine**, 2004. **38**(3): p. 248-249.
4. FitzGerald, G. and E. Ricciotti, **Prostaglandins and Inflammation**. Arterioscler Thromb Vasc Biol, 2011. **31**(5): p. 986-1000.
5. Nathan, C., **Points of control in inflammation**. Nature, 2002. **420**(6917): p. 846.
6. Yuan, C., et al., *Cyclooxygenase allostereism, fatty acid-mediated cross-talk between monomers of cyclooxygenase homodimers*. **Journal of Biological Chemistry**, 2009. **284**(15): p. 10046-10055.
7. McAdam, B., et al., *Effect of regulated expression of human cyclooxygenase isoforms on eicosanoid and isoeicosanoid production in inflammation*. **The Journal of clinical investigation**, 2000. **105**(10): p. 1473-1482.

8. Rainsford, K., **Anti-inflammatory drugs in the 21st century, in Inflammation in the pathogenesis of chronic diseases.** 2007, Springer. p. 3-27.
9. Wongrakpanich, S., et al., **A comprehensive review of non-steroidal anti-inflammatory drug use in the elderly.** Aging and disease, 2018. **9**(1): p. 143.
10. Badri, W., et al., *Encapsulation of NSAIDs for inflammation management: overview, progress, challenges and prospects.* **International journal of pharmaceutics**, 2016. **515**(1-2): p. 757-773.
11. Hochberg, M.C., et al., **American College of Rheumatology 2012 recommendations for the use of nonpharmacologic and pharmacologic therapies in osteoarthritis of the hand, hip, and knee.** Arthritis care & research, 2012. **64**(4): p. 465-474.
12. Sostres, C., et al., **Adverse effects of non-steroidal anti-inflammatory drugs (NSAIDs, aspirin and coxibs) on upper gastrointestinal tract.** Best practice & research Clinical gastroenterology, 2010. **24**(2): p. 121-132.
13. Higuchi, K., et al., *Present status and strategy of NSAIDs-induced small bowel injury.* **Journal of gastroenterology**, 2009. **44**(9): p. 879-888.

14. Lanas, A., M. Boers, and J. Nuevo, **Gastrointestinal events in at-risk patients starting non-steroidal anti-inflammatory drugs (NSAIDs) for rheumatic diseases: the EVIDENCE study of European routine practice**. *Annals of the rheumatic diseases*, 2015. **74**(4): p. 675-681.
15. Sigthorsson, G., et al., **COX-1 and 2, intestinal integrity, and pathogenesis of nonsteroidal anti-inflammatory drug enteropathy in mice**. *Gastroenterology*, 2002. **122**(7): p. 1913-1923.
16. Okyar, A., Y. Özsoy, and S. Güngör, **Novel formulation approaches for dermal and transdermal delivery of non-steroidal anti-inflammatory drugs**. *Rheumatoid arthritis—Treatment*. Rijeka: InTech, 2012: p. 25-48.
17. Ziltener, J.-L., S. Leal, and P.-E. Fournier, **Non-steroidal anti-inflammatory drugs for athletes: an update**. *Annals of physical and rehabilitation medicine*, 2010. **53**(4): p. 278-288.
18. Kim, S.J., A.J. Flach, and L.M. Jampol, **Nonsteroidal anti-inflammatory drugs in ophthalmology**. *Survey of ophthalmology*, 2010. **55**(2): p. 108-133.
19. Rostom, A., et al., **Prevention of NSAID- induced gastroduodenal ulcers**. *Cochrane database of systematic reviews*, 2002(4).
20. Vandraas, K.F., et al., *Non-steroidal anti-inflammatory drugs: use and co-treatment with potentially interacting medications in the elderly*. *European journal of clinical pharmacology*, 2010. **66**(8): p. 823-829.

21. Stillman, M.J. and M.T. Stillman, **Appropriate use of NSAIDs: considering cardiovascular risk in the elderly**. Geriatrics (Basel, Switzerland), 2007. **62**(3): p. 16-21.
22. Amadio Jr, P., D.M. Cummings, and P.B. Amadio, **NSAIDs revisited: selection, monitoring, and safe use**. Postgraduate medicine, 1997. **101**(2): p. 257-271.
23. Rainsford, K., *Profile and mechanisms of gastrointestinal and other side effects of nonsteroidal anti-inflammatory drugs (NSAIDs)*. The American journal of medicine, 1999. **107**(6): p. 27-35.
24. Woessner, K.M. and M. Castells, **NSAID Single-Drug–Induced Reactions**. Immunology and Allergy Clinics, 2013. **33**(2): p. 237-249.
25. Fokunang, C., et al., **Overview of Non-Steroidal Anti-Inflammatory Drugs (NSAIDs) in Resource Limited Countries**. MOJ Toxicol, 2018. **4**(1): p. 00081.
26. Yeh, K.C., *Pharmacokinetic overview of indomethacin and sustained-release indomethacin*. The American journal of medicine, 1985. **79**(4): p. 3-12.
27. Fritsche, E., et al., *Functional characterization of cyclooxygenase-2 polymorphisms*. Journal of Pharmacology and Experimental Therapeutics, 2001. **299**(2): p. 468-476.

28. Clarysse, S., et al., **Postprandial changes in solubilizing capacity of human intestinal fluids for BCS class II drugs**. *Pharmaceutical research*, 2009. **26**(6): p. 1456-1466.
29. Gallo, O., et al., **Cyclooxygenase-2 pathway correlates with VEGF expression in head and neck cancer**. Implications for tumor angiogenesis and metastasis. *Neoplasia*, 2001. **3**(1): p. 53-61.
30. Farrag, A.M., **Synthesis and Biological Evaluation of Novel Indomethacin Derivatives as Potential Anti- Colon Cancer Agents**. *Archiv der Pharmazie*, 2016. **349**(12): p. 904-914.
31. Brunelli, C., et al., *The non-steroidal anti-inflammatory drug indomethacin activates the eIF2 $\alpha$  kinase PKR, causing a translational block in human colorectal cancer cells*. *Biochemical Journal*, 2012. **443**(2): p. 379-386.
32. Hojka-Osinska, A., E. Ziolo, and A. Rapak, **Combined treatment with fenretinide and indomethacin induces AIF-mediated, non-classical cell death in human acute T-cell leukemia Jurkat cells**. *Biochemical and biophysical research communications*, 2012. **419**(3): p. 590-595.
33. Johannesdottir, S.A., et al., **Nonsteroidal anti- inflammatory drugs and the risk of skin cancer: a population- based case- control study**. *Cancer*, 2012. **118**(19): p. 4768-4776.

34. Zarghi, A. and S. Arfaei, *Selective COX-2 inhibitors: a review of their structure-activity relationships*. Iranian journal of pharmaceutical research: IJPR, 2011. **10**(4): p. 655.
35. Saeedi, M., et al., *Enhancement of dissolution rate of indomethacin: Using liquisolid compacts*. Iranian journal of pharmaceutical research: IJPR, 2011. **10**(1): p. 25.
36. Alsaidan, S.M., A.A. Alsughayer, and A.G. Eshra, **Improved dissolution rate of indomethacin by adsorbents**. Drug development and industrial pharmacy, 1998. **24**(4): p. 389-394.
37. Lucas, S., *The pharmacology of indomethacin. Headache: The Journal of Head and Face Pain*, 2016. **56**(2): p. 436-446.
38. Berlin, R.G., B.V. Clineschmidt, and J.A. Majka, *Famotidine: an appraisal of its mode of action and safety*. The American journal of medicine, 1986. **81**(4): p. 8-12.
39. Talke, P.O. and D.R. Solanki, **Dose-response study of oral famotidine for reduction of gastric acidity and volume in outpatients and inpatients**. Anesthesia and analgesia, 1993. **77**(6): p. 1143-1148.
40. McCullough, A.J., et al., **Suppression of nocturnal acid secretion with famotidine accelerates gastric ulcer healing**. Gastroenterology, 1989. **97**(4): p. 860-866.

41. Vinayek, R., et al., *Famotidine in the therapy of gastric hypersecretory states*. The American journal of medicine, 1986. **81**(4): p. 49-59.
42. Keithley, J., **Histamine H<sub>2</sub>-receptor antagonists**. The Nursing clinics of North America, 1991. **26**(2): p. 361-373.
43. Hudson, N., et al., **Famotidine for healing and maintenance in nonsteroidal anti-inflammatory drug-associated gastroduodenal ulceration**. Gastroenterology, 1997. **112**(6): p. 1817-1822.
44. Naito, Y., et al., *Prevention of indomethacin-induced gastric mucosal injury in Helicobacter pylori-negative healthy volunteers: a comparison study rebamipide vs famotidine*. Journal of clinical biochemistry and nutrition, 2008. **43**(1): p. 34-40.
45. Perez-Aisa, A., et al., **Effect of exogenous administration of transforming growth factor-beta and famotidine on the healing of duodenal ulcer under the impact of indomethacin**. Digestive and liver disease, 2003. **35**(6): p. 397-403.
46. Hassan, M.A., et al., *Characterization of famotidine polymorphic forms*. International journal of pharmaceutics, 1997. **149**(2): p. 227-232.
47. Ong, C.K., et al., **Combining paracetamol (acetaminophen) with nonsteroidal antiinflammatory drugs: a qualitative systematic review of analgesic efficacy for acute postoperative pain**. Anesthesia & Analgesia, 2010. **110**(4): p. 1170-1179.

48. Jordan, K., et al., EULAR Recommendations 2003: **an evidence based approach to the management of knee osteoarthritis: Report of a Task Force of the Standing Committee for International Clinical Studies Including Therapeutic Trials (ESCISIT)**. *Annals of the rheumatic diseases*, 2003. **62**(12): p. 1145-1155.
49. Blieden, M., et al., **A perspective on the epidemiology of acetaminophen exposure and toxicity in the United States**. *Expert review of clinical pharmacology*, 2014. **7**(3): p. 341-348.
50. Graham, G.G. and K.F. Scott, *Mechanism of action of paracetamol*. *American journal of therapeutics*, 2005. **12**(1): p. 46-55.
51. Graham, G.G., et al., **The modern pharmacology of paracetamol: therapeutic actions, mechanism of action, metabolism, toxicity and recent pharmacological findings**. *Inflammopharmacology*, 2013. **21**(3): p. 201-232.
52. Baek, J.-S., et al., **Controlled-release nanoencapsulating microcapsules to combat inflammatory diseases**. *Drug Design, Development and Therapy*, 2017. **11**: p. 1707.
53. Baek, J.-S. and C.-W. Cho, *Controlled release and reversal of multidrug resistance by co-encapsulation of paclitaxel and verapamil in solid lipid nanoparticles*. *International journal of pharmaceutics*, 2015. **478**(2): p. 617-624.



54. Coradini, K., et al., *A novel approach to arthritis treatment based on resveratrol and curcumin co-encapsulated in lipid-core nanocapsules: in vivo studies*. **European Journal of Pharmaceutical Sciences**, 2015. **78**: p. 163-170.
55. Freeling, J.P., et al., **Long-acting three-drug combination anti-HIV nanoparticles enhance drug exposure in primate plasma and cells within lymph nodes and blood**. **AIDS (London, England)**, 2014. **28**(17): p. 2625.
56. Feynman, R.P., **There's plenty of room at the bottom**. **California Institute of Technology**, Engineering and Science magazine, 1960.
57. Khan, I., K. Saeed, and I. Khan, *Nanoparticles: Properties, applications and toxicities*. **Arabian Journal of Chemistry**, 2019. **12**(7): p. 908-931.
58. Ealias, A.M. and M. Saravanakumar. **A review on the classification, characterisation, synthesis of nanoparticles and their application**. in **IOP Conf. Ser. Mater. Sci. Eng.** 2017.
59. Jeevanandam, J., et al., *Review on nanoparticles and nanostructured materials: history, sources, toxicity and regulations*. **Beilstein journal of nanotechnology**, 2018. **9**(1): p. 1050-1074.
60. Heera, P. and S. Shanmugam, *Nanoparticle characterization and application: an overview*. **Int. J. Curr. Microbiol. App. Sci**, 2015. **4**(8): p. 379-386.

61. Nair, L.S. and C.T. Laurencin, **Biodegradable polymers as biomaterials**. Progress in polymer science, 2007. **32**(8-9): p. 762-798.
62. Uhrich, K.E., et al., **Polymeric systems for controlled drug release**. Chemical reviews, 1999. **99**(11): p. 3181-3198.
63. Khoei, S. and M. Yaghoobian, *An investigation into the role of surfactants in controlling particle size of polymeric nanocapsules containing penicillin-G in double emulsion*. European journal of medicinal chemistry, 2009. **44**(6): p. 2392-2399.
64. Gupta, A. and V. Kumar, *New emerging trends in synthetic biodegradable polymers–Polylactide: A critique*. European polymer journal, 2007. **43**(10): p. 4053-4074.
65. Park, J.-H., M.G. Allen, and M.R. Prausnitz, *Biodegradable polymer microneedles: fabrication, mechanics and transdermal drug delivery*. Journal of controlled release, 2005. **104**(1): p. 51-66.
66. Pisani, E., et al., **Tuning microcapsules surface morphology using blends of homo-and copolymers of PLGA and PLGA-PEG**. Soft Matter, 2009. **5**(16): p. 3054-3060.
67. Wang, K., S. Strandman, and X. Zhu, **A mini review: Shape memory polymers for biomedical applications**. Frontiers of Chemical Science and Engineering, 2017. **11**(2): p. 143-153.

68. El-Hadi, A.M., **Miscibility of crystalline/amorphous/crystalline biopolymer blends from PLLA/PDLLA/PHB with additives**. Polymer-Plastics Technology and Materials, 2019. **58**(1): p. 31-39.
69. Auras, R., B. Harte, and S. Selke, **An overview of polylactides as packaging materials**. Macromolecular bioscience, 2004. **4**(9): p. 835-864.
70. Saeidlou, S., et al., **Poly (lactic acid) crystallization**. Progress in Polymer Science, 2012. **37**(12): p. 1657-1677.
71. Lin, Y., et al., ***Biocompatibility of poly-DL-lactic acid (PDLLA) for lung tissue engineering***. Journal of biomaterials applications, 2006. **21**(2): p. 109-118.
72. Bouissou, C., et al., **The influence of surfactant on PLGA microsphere glass transition and water sorption: remodeling the surface morphology to attenuate the burst release**. Pharmaceutical research, 2006. **23**(6): p. 1295-1305.
73. Makadia, H.K. and S.J. Siegel, **Poly lactic-co-glycolic acid (PLGA) as biodegradable controlled drug delivery carrier**. Polymers, 2011. **3**(3): p. 1377-1397.
74. Guarino, V., et al., **Polycaprolactone: Synthesis, properties, and applications**. Encyclopedia of Polymer Science and Technology, 2017: p. 1-36.

75. Woodruff, M.A. and D.W. Hutmacher, **The return of a forgotten polymer—Polycaprolactone in the 21st century**. *Progress in polymer science*, 2010. **35**(10): p. 1217-1256.
76. Amoozgar, Z. and Y. Yeo, **Recent advances in stealth coating of nanoparticle drug delivery systems**. *Wiley Interdisciplinary Reviews: Nanomedicine and Nanobiotechnology*, 2012. **4**(2): p. 219-233.
77. Li, S.-D. and L. Huang, *Stealth nanoparticles: high density but sheddable PEG is a key for tumor targeting*. *Journal of controlled release: official journal of the Controlled Release Society*, 2010. **145**(3): p. 178.
78. Nagavarma, B., et al., *Different techniques for preparation of polymeric nanoparticles-a review*. *Asian J. Pharm. Clin. Res*, 2012. **5**(3): p. 16-23.
79. Kita, K. and C. Dittrich, **Drug delivery vehicles with improved encapsulation efficiency: taking advantage of specific drug-carrier interactions**. *Expert opinion on drug delivery*, 2011. **8**(3): p. 329-342.
80. Peer, D., et al., **Nanocarriers as an emerging platform for cancer therapy**. *Nature nanotechnology*, 2007. **2**(12): p. 751.
81. Al-Lawati, H., Z. Binkhathlan, and A. Lavasanifar, *Nanomedicine for the effective and safe delivery of non-steroidal anti-inflammatory drugs: a review of preclinical research*. *European Journal of Pharmaceutics and Biopharmaceutics*, 2019.

82. ud Din, F., et al., *Effective use of nanocarriers as drug delivery systems for the treatment of selected tumors*. **International journal of nanomedicine**, 2017. **12**: p. 7291.
83. Rivas, C.J.M., et al., *Nanoprecipitation process: From encapsulation to drug delivery*. **International journal of pharmaceutics**, 2017. **532**(1): p. 66-81.
84. Fessi, H., et al., *Nanocapsule formation by interfacial polymer deposition following solvent displacement*. **International journal of pharmaceutics**, 1989. **55**(1): p. R1-R4.
85. Miladi, K., et al., **Nanoprecipitation process: from particle preparation to in vivo applications**, in *Polymer Nanoparticles for Nanomedicines*. 2016, Springer. p. 17-53.
86. Paliwal, R., R.J. Babu, and S. Palakurthi, **Nanomedicine scale-up technologies: feasibilities and challenges**. *Aaps Pharmscitech*, 2014. **15**(6): p. 1527-1534.
87. Feeney, O.M., et al., **50 years of oral lipid-based formulations: provenance, progress and future perspectives**. *Advanced drug delivery reviews*, 2016. **101**: p. 167-194.
88. Gursoy, R.N. and S. Benita, **Self-emulsifying drug delivery systems (SEDDS) for improved oral delivery of lipophilic drugs**. *Biomedicine & Pharmacotherapy*, 2004. **58**(3): p. 173-182.

89. Mohsin, K., M.A. Long, and C.W. Pouton, *Design of lipid- based formulations for oral administration of poorly water- soluble drugs: precipitation of drug after dispersion of formulations in aqueous solution*. **Journal of pharmaceutical sciences**, 2009. **98**(10): p. 3582-3595.
90. McClements, D.J., **Nanoemulsions versus microemulsions: terminology, differences, and similarities**. *Soft matter*, 2012. **8**(6): p. 1719-1729.
91. McClements, D.J., **Edible nanoemulsions: fabrication, properties, and functional performance**. *Soft Matter*, 2011. **7**(6): p. 2297-2316.
92. Rehman, F.U., et al., **From nanoemulsions to self-nanoemulsions, with recent advances in self-nanoemulsifying drug delivery systems (SNEDDS)**. *Expert opinion on drug delivery*, 2017. **14**(11): p. 1325-1340.
93. Jaiswal, M., R. Dudhe, and P. Sharma, **Nanoemulsion: an advanced mode of drug delivery system**. *3 Biotech*, 2015. **5**(2): p. 123-127.
94. Sainsbury, F., B. Zeng, and A.P. Middelberg, **Towards designer nanoemulsions for precision delivery of therapeutics**. *Current opinion in chemical engineering*, 2014. **4**: p. 11-17.
95. Bernardi, D.S., et al., *Formation and stability of oil-in-water nanoemulsions containing rice bran oil: in vitro and in vivo assessments*. **Journal of nanobiotechnology**, 2011. **9**(1): p. 44.

96. Kumar, M., et al., **Techniques for Formulation of Nanoemulsion Drug Delivery System: A Review**. Preventive nutrition and food science, 2019. **24**(3): p. 225.
97. Jafari, S., B. Bhandari, and Y. He. **Optimization of nano-emulsion production by sonication and microfluidization. in Chemeca 2005, 33rd Australasian Chemical Engineering Conference**. 2005. Institute of Engineers, Australia, IChemE in Australia, SCENZ and RACI in ....
98. Gonçalves, A., et al., **Production, properties, and applications of solid self-emulsifying delivery systems (S-SEDS) in the food and pharmaceutical industries**. Colloids and Surfaces A: Physicochemical and Engineering Aspects, 2018. **538**: p. 108-126.
99. Graves, S., et al., *Structure of concentrated nanoemulsions*. **The Journal of chemical physics**, 2005. **122**(13): p. 134703.
100. Leong, T., et al., **Minimising oil droplet size using ultrasonic emulsification**. Ultrasonics sonochemistry, 2009. **16**(6): p. 721-727.
101. Mahdi Jafari, S., Y. He, and B. *Bhandari*, **Nano-emulsion production by sonication and microfluidization—a comparison**. **International Journal of Food Properties**, 2006. **9**(3): p. 475-485.
102. Salvia-Trujillo, L., et al., **Impact of microfluidization or ultrasound processing on the antimicrobial activity against Escherichia coli of lemongrass oil-loaded nanoemulsions**. Food Control, 2014. **37**: p. 292-297.

103. Tiwari, S., D. Shenoy, and M. Amiji, **Nanoemulsion formulations for improved oral delivery of poorly soluble drugs**. *Nanotech*, 2006. **1**: p. 475-8.
104. Singh, Y., et al., *Nanoemulsion: Concepts, development and applications in drug delivery*. *Journal of Controlled Release*, 2017. **252**: p. 28-49.
105. Assali, M., et al., *Preparation and characterization of carvedilol-loaded poly (d, l) lactide nanoparticles/microparticles as a sustained-release system*. *International Journal of Polymeric Materials and Polymeric Biomaterials*, 2017. **66**(14): p. 717-725.
106. Assali, M., et al., *Dexamethasone-diclofenac loaded polylactide nanoparticles: Preparation, release and anti-inflammatory activity*. *European Journal of Pharmaceutical Sciences*, 2018. **122**: p. 179-184.
107. Bernardi, A., et al., *Effects of indomethacin- loaded nanocapsules in experimental models of inflammation in rats*. *British journal of pharmacology*, 2009. **158**(4): p. 1104-1111.
108. Bernardi, A., et al., *Indomethacin-loaded lipid-core nanocapsules reduce the damage triggered by A $\beta$ 1-42 in Alzheimer's disease models*. *International journal of nanomedicine*, 2012. **7**: p. 4927.



109. Wei, X., et al., **Thermosensitive  $\beta$ -cyclodextrin modified poly ( $\epsilon$ -caprolactone)-poly (ethylene glycol)-poly ( $\epsilon$ -caprolactone) micelles prolong the anti-inflammatory effect of indomethacin following local injection.** *Acta biomaterialia*, 2013. **9**(6): p. 6953-6963.
110. Yokota, J. and S. Kyotani, *Influence of nanoparticle size on the skin penetration, skin retention and anti-inflammatory activity of non-steroidal anti-inflammatory drugs.* *Journal of the Chinese Medical Association*, 2018. **81**(6): p. 511-519.
111. Nagai, N., C. Yoshioka, and Y. Ito, *Topical therapies for rheumatoid arthritis by gel ointments containing indomethacin nanoparticles in adjuvant-induced arthritis rat.* *Journal of oleo science*, 2015. **64**(3): p. 337-346.
112. Puglia, C., et al., *Evaluation of in - vivo topical anti - inflammatory activity of indometacin from liposomal vesicles.* *Journal of pharmacy and pharmacology*, 2004. **56**(10): p. 1225-1232.
113. Nagai, N., et al., **A nanoparticle formulation reduces the corneal toxicity of indomethacin eye drops and enhances its corneal permeability.** *Toxicology*, 2014. **319**: p. 53-62.
114. Nagai, N. and Y. Ito, **Effect of solid nanoparticle of indomethacin on therapy for rheumatoid arthritis in adjuvant-induced arthritis rat.** *Biological and Pharmaceutical Bulletin*, 2014. **37**(7): p. 1109-1118.

115. Chandrasekar, D., et al., *Folate coupled poly (ethyleneglycol) conjugates of anionic poly (amidoamine) dendrimer for inflammatory tissue specific drug delivery*. **Journal of Biomedical Materials Research Part A**, 2007. **82**(1): p. 92-103.
116. Soehngen, E.C., et al., *Encapsulation of indomethacin in liposomes provides protection against both gastric and intestinal ulceration when orally administered to rats*. **Arthritis & Rheumatism: Official Journal of the American College of Rheumatology**, 1988. **31**(3): p. 414-422.
117. Rosset, V., et al., *Elaboration of argan oil nanocapsules containing naproxen for cosmetic and transdermal local application*. **Journal of Colloid Science and Biotechnology**, 2012. **1**(2): p. 218-224.
118. Hornig, S., H. Bunjes, and T. Heinze, *Preparation and characterization of nanoparticles based on dextran–drug conjugates*. **Journal of colloid and interface science**, 2009. **338**(1): p. 56-62.
119. Mora-Huertas, C.E., et al., *Nanocapsules prepared via nanoprecipitation and emulsification–diffusion methods: Comparative study*. **European Journal of Pharmaceutics and Biopharmaceutics**, 2012. **80**(1): p. 235-239.
120. Lenz, Q.F., et al., *Semi-solid topical formulations containing nimesulide-loaded nanocapsules showed in-vivo anti-inflammatory activity in chronic arthritis and fibrovascular tissue models*. **Inflammation Research**, 2012. **61**(4): p. 305-310.

121. Badri, W., et al., *Elaboration of nanoparticles containing indomethacin: Argan oil for transdermal local and cosmetic application*. **Journal of Nanomaterials**, 2015. **16**(1): p. 113.
122. Badri, W., et al., **Polycaprolactone based nanoparticles loaded with indomethacin for anti-inflammatory therapy: from preparation to ex vivo study**. *Pharmaceutical research*, 2017. **34**(9): p. 1773-1783.
123. Závášová, V., et al., *Encapsulation of indomethacin in magnetic biodegradable polymer nanoparticles*. **Journal of magnetism and magnetic materials**, 2007. **311**(1): p. 379-382.
124. El-Leithy, E.S., H.K. Ibrahim, and R.M. Sorour, **In vitro and in vivo evaluation of indomethacin nanoemulsion as a transdermal delivery system**. *Drug delivery*, 2015. **22**(8): p. 1010-1017.
125. Kwasigroch, B., et al., *Oil-in-water nanoemulsions are suitable for carrying hydrophobic compounds: Indomethacin as a model of anti-inflammatory drug*. **International journal of pharmaceutics**, 2016. **515**(1-2): p. 749-756.
126. Rodríguez-Burneo, N., M. Busquets, and J. Estelrich, **Magnetic nanoemulsions: comparison between nanoemulsions formed by ultrasonication and by spontaneous emulsification**. *Nanomaterials*, 2017. **7**(7): p. 190.
127. 7.0, E.P., 4.1.3. **Buffer solutions**. 2011.

128. Li, P.-H. and B.-H. Chiang, **Process optimization and stability of D-limonene-in-water nanoemulsions prepared by ultrasonic emulsification using response surface methodology**. *Ultrasonics sonochemistry*, 2012. **19**(1): p. 192-197.
129. Assali, M., et al., ***RP-HPLC Method Development and Validation of Synthesized Codrug in Combination with Indomethacin, Paracetamol, and Famotidine***. *International Journal of Analytical Chemistry*. 2020.
130. Ravisankar, P., et al., ***A review on step-by-step analytical method validation***. *IOSR J Pharm*, 2015. **5**(10): p. 7-19.
131. Abualhasan, M.N., **A Validated Stability-Indicating HPLC Method for Routine Analysis of an Injectable Lincomycin and Spectinomycin Formulation**. *Scientia Pharmaceutica*, 2012. **80**(4): p. 977-986.
132. Costa, P. and J.M.S. Lobo, ***Modeling and comparison of dissolution profiles***. *European journal of pharmaceutical sciences*, 2001. **13**(2): p. 123-133.
133. Akaike, H., **A new look at the statistical model identification**. *IEEE transactions on automatic control*, 1974. **19**(6): p. 716-723.
134. Aljuffali, I.A., et al., **The codrug approach for facilitating drug delivery and bioactivity**. *Expert opinion on drug delivery*, 2016. **13**(9): p. 1311-1325.

135. Das, N., et al., *Codrug: an efficient approach for drug optimization*. **European Journal of Pharmaceutical Sciences**, 2010. **41**(5): p. 571-588.
136. Hessien, M., et al., **Stability and tunability of O/W nanoemulsions prepared by phase inversion composition**. *Langmuir*, 2011. **27**(6): p. 2299-2307.
137. Koroleva, M., T. Nagovitsina, and E. Yurtov, **Nanoemulsions stabilized by non-ionic surfactants: stability and degradation mechanisms**. *Physical Chemistry Chemical Physics*, 2018. **20**(15): p. 10369-10377.
138. Suyanto, A., et al. **Nano-Emulsion and Nano-Encapsulation of Fruit Flavor**. in *IOP Conference Series: Earth and Environmental Science*. 2019. IOP Publishing.
139. Gerhäuser, C., et al., **Mechanism-based in vitro screening of potential cancer chemopreventive agents**. *Mutation Research/Fundamental and Molecular Mechanisms of Mutagenesis*, 2003. **523**: p. 163-172.
140. Bhattacharjee, S., *DLS and zeta potential—what they are and what they are not?* **Journal of Controlled Release**, 2016. **235**: p. 337-351.
141. Moraes, T.M., et al., *Healing actions of essential oils from Citrus aurantium and d-limonene in the gastric mucosa: the roles of VEGF, PCNA, and COX-2 in cell proliferation*. **Journal of medicinal food**, 2013. **16**(12): p. 1162-1167.

142. de Souza, M.C., et al., **Gastroprotective effect of limonene in rats: Influence on oxidative stress, inflammation and gene expression.** *Phytomedicine*, 2019. **53**: p. 37-42.
143. Torchilin, V.P. and V.S. Trubetskoy, **Which polymers can make nanoparticulate drug carriers long-circulating?** *Advanced drug delivery reviews*, 1995. **16**(2-3): p. 141-155.
144. Sawalha, H., et al., ***Poly lactide microspheres prepared by premix membrane emulsification—Effects of solvent removal rate.*** *Journal of membrane science*, 2008. **310**(1-2): p. 484-493.
145. Guideline, I.H.T. **Validation of analytical procedures: text and methodology Q2 (R1).** in International conference on harmonization, Geneva, Switzerland. 2005.
146. Assali, M., et al., ***RP-HPLC Method Development and Validation of Synthesized Codrug in Combination with Indomethacin, Paracetamol, and Famotidine.*** *International Journal of Analytical Chemistry*, 2020. **2020**.
147. Abualhasan, M., et al., Synthesis, **Formulation and Analytical Method Validation of Rutin Derivative.** *Letters in Drug Design & Discovery*, 2019. **16**(6): p. 685-695.
148. Handbook, S.U., **Micromath.** Inc., Salt Lake City, UT, 1995. **467**.

149. Costa, F., et al., *Comparison of dissolution profiles of Ibuprofen pellets*. **Journal of controlled release**, 2003. **89**(2): p. 199-212.
150. Koizumi, T., G.C. Ritthidej, and T. *Phaechamud*, *Mechanistic modeling of drug release from chitosan coated tablets*. **Journal of controlled release**, 2001. **70**(3): p. 277-284.
151. Mayer, B.X., et al., *Pharmacokinetic- pharmacodynamic profile of systemic nitric oxide- synthase inhibition with L- NMMA in humans*. **British journal of clinical pharmacology**, 1999. **47**(5): p. 539-544.
152. Makoid, M., A. Dufour, and U. Banakar, **Modelling of dissolution behaviour of controlled release system**. *STP pharma pratiques*, 1993. **3**: p. 49-49.
153. Sharma, R., R.B. Walker, and K. Pathak, *Evaluation of the kinetics and mechanism of drug release from econazole nitrate nanosponge loaded carboxypol hydrogel*. **Indian journal of pharmaceutical education and research**, 2011. **45**(1): p. 25-31.
154. Kumar, V., et al., *Application of assumed IVIVC in product life cycle management: a case study of trimetazidine dihydrochloride extended release tablet*. **J. Bioequiv. Bioavailab**, 2013. **5**(1): p. 6-15.
155. Kosmidis, K., P. Argyrakakis, and P. Macheras, **A reappraisal of drug release laws using Monte Carlo simulations: the prevalence of the Weibull function**. *Pharmaceutical research*, 2003. **20**(7): p. 988-995.

156. Ignacio, M., M.V. Chubynsky, and G.W. Slater, **Interpreting the Weibull fitting parameters for diffusion-controlled release data**. Physica A: Statistical Mechanics and its Applications, 2017. **486**: p. 486-496.
157. De, S. and D.H. Robinson, **Particle size and temperature effect on the physical stability of PLGA nanospheres and microspheres containing Bodipy**. Aaps Pharmscitech, 2004. **5**(4): p. 18-24.
158. Mdzinarashvili, T., et al., *Stability of various PLGA and lipid nanoparticles in temperature and in time and new technology for the preparation of liposomes for anticancer and antibiotic loading*. Journal of Thermal Analysis and Calorimetry: p. 1-10.
159. Díaz, E., I. Sandonis, and M.B. Valle, *In vitro degradation of poly (caprolactone)/nHA composites*. Journal of Nanomaterials, 2014. **2014**: p. 185.



## Appendix

### Appendix A: RP-HPLC Method Development and Validation of Synthesized Codrug in Combination with Indomethacin, Paracetamol, and Famotidine article.

Hindawi  
International Journal of Analytical Chemistry  
Volume 2020, Article ID 1894907, 9 pages  
<https://doi.org/10.1155/2020/1894907>



#### Research Article

### RP-HPLC Method Development and Validation of Synthesized Codrug in Combination with Indomethacin, Paracetamol, and Famotidine

Mohyeddin Assali , Murad Abualhasan , Nihal Zohud , and Noura Ghazal

Department of Pharmacy, Faculty of Medicine and Health Sciences, An-Najah National University, P.O. Box 7, Nablus, State of Palestine

Correspondence should be addressed to Mohyeddin Assali; m.d.assali@najah.edu

Received 24 March 2020; Revised 31 May 2020; Accepted 11 June 2020; Published 1 July 2020

Academic Editor: Antonio V. Herrera-Herrera

Copyright © 2020 Mohyeddin Assali et al. This is an open access article distributed under the Creative Commons Attribution License, which permits unrestricted use, distribution, and reproduction in any medium, provided the original work is properly cited.

**Background.** Indomethacin is considered a potent nonsteroidal anti-inflammatory drug that could be combined with Paracetamol to have superior and synergist activity to manage pain and inflammation. To reduce the gastric side effect, they could be combined with Famotidine. **Methodology.** A codrug of Indomethacin and Paracetamol was synthesized and combined in solution with Famotidine. The quantification of the pharmaceutically active ingredients is pivotal in the development of pharmaceutical formulations. Therefore, a novel reverse-phase high-performance liquid chromatography (RP-HPLC) method was developed and validated according to the International Council for Harmonization (ICH) Q2R1 guidelines. A reverse phase C18 column with a mobile phase acetonitrile: sodium acetate buffer 60:40 at a flow rate of 1.4 mL/min and pH 5 was utilized. **Results.** The developed method showed good separation of the four tested drugs with a linear range of 0.01–0.1 mg/mL ( $R^2 > 0.99$ ). The LODs for FAM, PAR, IND, and codrug were  $3.076 \times 10^{-9}$ ,  $3.868 \times 10^{-10}$ ,  $1.066 \times 10^{-9}$ , and  $4.402 \times 10^{-9}$  mg/mL respectively. While the LOQs were  $9.322 \times 10^{-9}$ ,  $1.172 \times 10^{-10}$ ,  $3.232 \times 10^{-9}$ , and  $1.334 \times 10^{-8}$  mg/mL, respectively. Furthermore, the method was precise, accurate, selective, and robust with values of relative standard deviation (RSD) less than 2%. Moreover, the developed method was applied to study the *in vitro* hydrolysis and conversion of codrug into Indomethacin and Paracetamol. **Conclusion.** The codrug of Indomethacin and Paracetamol was successfully synthesized for the first time. Moreover, the developed analytical method, to our knowledge, is the first of its kind to simultaneously quantify four solutions containing the following active ingredients of codrug, Indomethacin, Paracetamol, and Famotidine mixture with added pharmaceutical inactive ingredients in one HPLC run.

#### 1. Introduction

Nonsteroidal anti-inflammatory drugs (NSAIDs) are among the most consumed and prescribed drugs for both pain and inflammation worldwide [1]. Their blockage of prostaglandin synthesis by inhibiting cyclooxygenase (COX) is responsible for both the desired anti-inflammatory effects and the undesired gastrointestinal effects [2–4]. Based on COX selectivity, NSAIDs are divided into two families: nonselective NSAIDs that block both cyclooxygenase I & II and selective cyclooxygenase II inhibitors [5–7].

Indomethacin (IND) is an example of a potent non-selective COX inhibitor that showed efficient analgesia with

antipyretic and anti-inflammatory activities [8]. It is classified as an indole-acetic acid derivative according to the NSAIDs chemical classification with the chemical name of 1-(*p*-chlorobenzoyl)-5-methoxy-2-methylindole-3-acetic acid [9]. It is a poorly soluble class II compound with a half-life of 4–5 h [10, 11]. It is utilized to treat rheumatoid diseases by elevating the inflammation. Moreover, it can decrease the risk of colon cancer by providing chemoprotective effects against tumors [12, 13]. Like other NSAIDs, it appeared to have gastrointestinal, renal, and other side effects [14]. The gastric side effect could be reversed by the administration of Famotidine (FAM), which is a competitive histamine H<sub>2</sub>-receptor antagonist that

inhibits the secretion of gastric acid and also increases collagen secretions [15, 16].

Recently, there has been a trend for combining NSAIDs with Paracetamol (PAR) as this often provides a synergic analgesic effect and reduces the adverse effects resulting from NSAIDs [17]. Paracetamol, *N*-acetyl-*p*-aminophenol (also known as acetaminophen), is utilized globally as an analgesic and antipyretic drug. Regarding the mechanism of action which is considered to be a weak inhibitor of the synthesis of prostaglandins (PGs), their effects *in vivo* are similar to these COX-2 inhibitors [18]. Although their analgesic effects are often weaker than NSAIDs, it has better tolerance, and accordingly, it is often preferred [19].

Indomethacin is considered strong and potent anti-inflammatory activity against rheumatoid arthritis and other inflammatory diseases and Paracetamol is considered as the first-choice medication for both acute and chronic pain [20]. Therefore, the combination of Indomethacin with Paracetamol provides excellent anti-inflammatory and analgesic activities with a reduction of the Indomethacin side effects. Seidman and Melander reported equianalgesic activity with milder side effects upon the administration of Paracetamol with a low dose of Indomethacin in comparison to the high dose of Indomethacin alone for the treatment of rheumatoid arthritis [21]. Famotidine is considered the most potent H<sub>2</sub> antagonist for the treatment of peptic ulcers and was found to be effective for prevention of Indomethacin-induced gastric injury even in the lowest dose [22, 23]. Therefore, we aim to synthesize a novel codrug of Indomethacin and Paracetamol (IND-PAR) through a hydrolyzable ester bond combined in solution with Famotidine.

Reverse phase-high performance chromatography (RP-HPLC) is considered one of the most common analytical techniques used for the development and characterization of pharmaceutical products [24, 25]. Moreover, HPLC provides a rapid, sensitive, and precise technique to separate and identify the analyzed drugs in combination or the used pharmaceutical dosage forms. Therefore, It is necessary to validate the developed HPLC method according to the International Council for Harmonization (ICH) and the United States Pharmacopeia (USP) requirements [26, 27].

Moreover, a simple and universal RP-HPLC method of analysis was developed and validated for the successful separation of a mixture containing four components: codrug, Indomethacin, Paracetamol, and Famotidine in the formulation. The developed method was used to study the hydrolysis profile of the codrug in the presence of the esterase enzyme.

## 2. Materials and Methods

**2.1. Materials and Reagents.** Indomethacin (IND), Famotidine (FAM), 4-(Dimethylamino) pyridine (DMAP), silica gel, and *N*-(3-Dimethylaminopropyl)-*N'*-ethylcarbodiimide hydrochloride (EDC) 98% were purchased from Sigma-Aldrich Company. Paracetamol (PAR) was purchased from Sun Pharma Ltd. (Nablus, Palestine). Sodium acetate trihydrate, disodium hydrogen phosphate, potassium

hydrogen phosphate, ethyl acetate 99.5% (EtOAc), hexane (Hex), and dichloromethane (DCM) were purchased from CS Company, Haifa. Acetonitrile supragradient grade for chromatography (ACN) and triethylamine (Et<sub>3</sub>N) were purchased from SDFCL. Porcine liver esterase (PLE) was purchased from Sigma-Aldrich, USA. Inactive pharmaceutical ingredients: microcrystalline cellulose, magnesium stearate, aerosol, and Ac-Di-Sol were donated by Jerusalem Pharmaceuticals Company, Palestine.

**2.2. Instrumentations.** High-Performance liquid chromatography (Waters 1525, Singapore) binary HPLC pump and waters 2298 photodiode Array Detector were used. Nuclear Magnetic Resonance (NMR) spectrum was recorded on Bruker 500 MHz-Avance III, Switzerland. The high-resolution mass spectrum (HRMS) was recorded on a Shimadzu LCMS-IT-TOF utilizing ESI (+) method.

**2.3. Synthesis of Indomethacin-Paracetamol (IND-PAR) Codrug.** Dichloromethane (8 mL) was added to a mixture of Indomethacin (200 mg, 0.60 mmol), Paracetamol (101.4 mg, 0.67 mmol), EDC (128.6 mg, 0.67 mmol), and DMAP (75.1 mg, 0.62 mmole) and was stirred at room temperature overnight under argon. The reaction was treated with DCM and 1 M HCl three times. The collected organic layers were evaporated using a rotary evaporator. Then the crude product was purified using flash chromatography on silica gel eluted with a mobile phase of Hex: EtOAc 1:2 to provide a yellow solid product with a yield 70% (220 mg) and *R<sub>f</sub>* = 0.63 (Hex: EtOAc 1:2). <sup>1</sup>H NMR (500 MHz, CDCl<sub>3</sub>): δ 2.11 (s, 3H, COCH<sub>3</sub>), 2.42 (s, 3H, CH<sub>3</sub> indole), 3.81 (s, 3H, OCH<sub>3</sub>), 3.86 (s, 2H, CH<sub>2</sub>CO), 6.68 (dd, 1H, *J* = 9.2 Hz, *J* = 2.3 Hz, H-7 indole), 6.68 (d, 1H, *J* = 9.2 Hz, H-9 indole), 6.98 (d, 2H, *J* = 8.8 Hz, phenyl), 7.02 (d, 1H, *J* = 2.3 Hz, H-6 indole), 7.45 (dd, 4H, *J* = 8.8 Hz, *J* = 1.9 Hz, phenyl), 7.65 (d, 2H, *J* = 8.4 Hz, phenyl). HRMS (ESI, *m/z*): calcd. for C<sub>27</sub>H<sub>24</sub>N<sub>2</sub>O<sub>5</sub>Cl [M + H]<sup>+</sup> 491.1374, found 491.1372.

## 2.4. HPLC Analytical Method Development

### 2.4.1. Prepared Solutions

(1) **Buffer Solution pH 6.** 13.6 g of sodium acetate trihydrate was dissolved in 750 mL HPLC water, then 1 mL of Et<sub>3</sub>N was added, diluted with HPLC water to 1 L, and adjusted to pH 6.0 with glacial acetic acid. The mobile phase was firstly prepared using a mixture of sodium acetate Buffer:ACN, 93:7 [28].

(2) **Diluent 1.** 6.8 g of potassium dihydrogen phosphate was dissolved in 1 L HPLC water and adjusted to a pH 6.0 using glacial acetic acid.

(3) **FAM, IND, PAR, and Codrug Standard Solutions.** 2.5 mg of the standard was weighed into 25 mL volumetric flask; 5 mL methanol was added and then diluted up to 25 mL by the prepared diluent.



(4) *Standard Solution Mixture*. 2.5 mg of each FAM, IND, PAR, and codrug was diluted with HPLC acetonitrile to the volume (25 mL).

2.4.2. *pH, Mobile Ratio, and Diluents Used in Method Development Trials*. Different mobile phase composition, pH, and diluents were tried throughout the analytical method development. The used mobile phases and diluents at different pH are summarized in Table 1.

2.5. *Analytical Method Validation*. The analytical method was developed according to USP and ICHQ2R1 guidelines and validated using the following parameters: linearity, range, accuracy, precision, robustness, and ruggedness [29]. All prepared parameters were in triplicates.

2.5.1. *Linearity and Range*. Linearity was measured by preparing a serial five concentrations in the range of 0.01–0.1 mg/mL from a preprepared stock solution of 1 mg/mL. The calibration curves were built by plotting the mean area under the curve (AUC) obtained from the HPLC against concentrations. The regression equation and the squared correlation coefficient ( $R^2$ ) were calculated for each ingredient curve.

2.5.2. *Accuracy*. Accuracy and selectivity validation parameters were calculated by preparing a standard solution of a mixture of four drugs, having a concentration of 0.24 mg/mL for each drug. Three concentration levels of 80%, 100%, and 120% of the standard concentration were made. The three solutions were prepared containing different excipients: microcrystalline cellulose, magnesium stearate, aerosol, and Ac-Di-Sol. The accuracy was evaluated by calculating the percentage of recovery.

2.5.3. *Selectivity*. The selectivity of the developed method was examined as the eluted peaks are well separated and not affected by any of the added excipients.

2.5.4. *Precision*. Precision was performed at different levels. At first, instrument precision was done by injecting the standard mixture 9 times; the % RSD of the generated peaks of the chromatogram was calculated. An intermediate precision including interday and between analyst precision was examined on 0.08 mg/mL and 0.1 mg/mL concentration, respectively. The percentage relative standard deviation was calculated for both mixtures.

2.5.5. *Robustness*. The robustness of the developed method was performed by doing minor modifications on the method parameters, including detection wavelength, different mobile phase pH, and flow rate [30]. The studied robustness parameters were the pH effect of the mobile phase (4.9, 5.0, and 5.1), the detection wavelength (273, 275, and 277 nm), and the effect of the mobile phase flow rate (1.2, and 1.4 mL/min).

TABLE 1: Summary of method development optimization.

Drug	Mobile phase		pH	Diluent used
	Buffer	ACN		
FAM and IND mixture	93	7	6	Diluent 1
	93	7	5	
	50	50	5.5	
	60	40	5.5 & 6	
	40	60	5.5 & 5	
Codrug	40	60	5	Diluent 1
PAR	40	60	5	Diluent 1 Methanol ACN
FAM, codrug, and IND separately	40	60	5	ACN
Mixture of all drugs	40	60	5	ACN

2.5.6. *Detection and Quantification Limit (LOD & LOQ)*. Limit of detection (LOD) and limit of quantification (LOQ) is an indication of the analytical method sensitivity. Signal to noise ratio in the HPLC chromatogram was used to calculate these two parameters for each compound. The LOD and LOQ value of the compound was determined when the signal to noise ratio is 3:1 and 1:10, respectively.

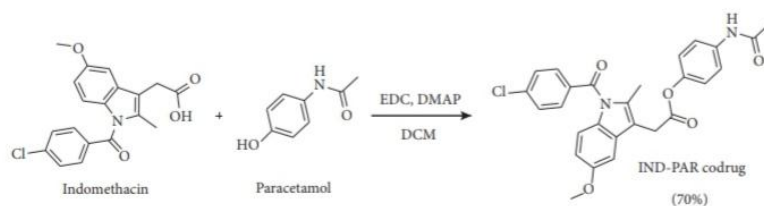
2.6. *Hydrolysis of Codrug*. The synthesized codrug was incubated with an esterase enzyme to study its hydrolysis to its parent drugs (IND & PAR). This was achieved by incubating 1 mg of codrug into 10 mL phosphate buffer saline solution (pH 7.4) containing 1 mg of esterase enzyme (10 U) at 37°C for 1 h [31–33]. At different time intervals, aliquots of 1 mL were obtained, and then the concentrations were analyzed by the developed HPLC method.

2.7. *Statistical Analysis*. All prepared parameters, including the *in vitro* hydrolysis of the codrug, were performed in triplicates. The data were expressed as means  $\pm$  relative standard deviation. Statistical analysis was performed on robustness parameters using the ANOVA test. Statistically, a significant difference was considered when the  $p$  value was  $<0.05$ .

### 3. Results and Discussion

3.1. *Synthesis of IND-PAR Codrug*. Herein, we aim to synthesize a codrug of Indomethacin and Paracetamol to obtain a synergistic analgesic, antipyretic, and anti-inflammatory activities. The synthesis of the codrug was achieved through the formation of the ester bond between IND and PAR using EDC as a coupling agent and 4-(Dimethylamino)pyridine as a base, as shown in Scheme 1. The codrug was successfully synthesized with a high yield of 70%. The structure of the codrug was confirmed by NMR and HRMS.

3.2. *Method Development*. The RP-HPLC analytical method for codrug, IND, PAR, and FAM was developed and validated according to the ICH guidelines [34]. The analytical method development was mainly based on the USP



SCHEME 1: Synthetic scheme of IND-PAR codrug.

analytical method of FAM and IND and was then optimized for the best separation for the component mixture [35].

At first, FAM and IND mixture was injected using the USP analytical method for the Famotidine tablet. The produced HPLC chromatogram showed only one peak of FAM, while the IND was not eluted even after 40 minutes. The late elution of IND is probably due to its high lipophilicity and the high hydrophobicity of the used mobile phase (ACN: sodium acetate buffer 7:93). Further modification of the mobile phase pH was done in order to reduce the retention time of IND by making the mobile phase more acidic. Different pH mobile phases were tried, including 5, 5.5, and 6. The results showed that the most acidic pH mobile (pH 5) achieved early elution of IND to less than 10 min. In order to get the best separation, the mobile phase was further optimized at different solvent compositions. Lastly, the best separation was achieved at the mobile phase composition (ACN: sodium acetate buffer 60:40). The codrug was added to the above mixture of IND and FAM using pure ACN as the diluent. The final HPLC chromatographic conditions of the developed method were by using XTERRA® MS C18, 5  $\mu$ m, 4.6  $\times$  250 mm analytical column with a flow rate of 1.4 mL/min and a detection wavelength of 275 nm. The operation temperature of the column was set at 25°C. The injection volume was 10  $\mu$ L and the run time was 20 minutes. The developed method showed well-separated peaks for the component mixture. The resulted peaks were symmetrical with narrow broadening eluted at different retention times: 3.220, 3.624, 7.751, and 14.034 min for FAM, PAR, IND, and codrug, respectively, as shown in Figure 1.

### 3.3. Method Validation

**3.3.1. Linearity and Range.** The quality of an analytical method is profoundly dependent on the linearity of the calibration curve. The main characteristics of a calibration curve are the slope line, the regression, and the correlation.

The linearity of the method was measured by plotting the area under the curve obtained from the HPLC of each drug against the corresponding concentrations. The linearity was demonstrated over the concentration range (0.01–0.1 mg/mL) for FAM, PAR, IND, and codrug, respectively. The obtained goodness-of-fit ( $R^2$ ) was more than 0.99 that confirms the linearity between the concentration and the area under the peak. The slopes of the regression line for FAM, PAR, IND, and codrug are shown in Figure 2.

**3.3.2. Selectivity.** The four drugs components (FAM, PAR, IND, and codrug) were formulated with the following inactive ingredients: microcrystalline cellulose, magnesium stearate, aerosol, and Ac-Di-Sol to study selectivity of the developed analytical method [36].

This parameter was investigated to show that there is no possible interference of the added tablet formula excipients on the separation and measurements of peak areas for the ingredient mixture (Figure 3).

**3.3.3. Accuracy.** The method showed great accuracy within the tested concentration range (0.08–0.12). The percentage of RSD and percentage of recovery for all tested solutions are within the acceptable limits ( $100\% \pm 2\%$ ); the data are shown in Table 2.

**3.3.4. Precision.** The precision of a method is the degree of agreement among individual test results when the procedure is applied repeatedly to multiple samplings.

The method precision was examined at different levels; system precision was examined by injecting 0.1 mg/mL nine times on HPLC and the % RSD was found to be less than 2.0 for all tested compounds.

The intermediate precision validation parameter at different days (intraday precision) was studied by performing three replicates measurements at two different concentrations (0.08 and 0.1 mg/mL). The results showed that the percentage relative standard deviation of the triplicate of each concentration was less than 2.0. Moreover, the repeatability was tested for different analysts by doing three replicates measurements of the mixture at 0.12 mg/mL and the result % RSD was also less than 2.0. The precision results at different precision levels are illustrated in Table 3.

### 3.3.5. Detection and Quantification Limit (LOD & LOQ).

The detection limit or LOD is the lowest amount of analyte in a sample that can be detected but not necessarily quantified. However, the limit of quantification or LOQ is the lowest amount of analyte in a sample that can be determined quantitatively with convenient precision and accuracy. The result showed that the calculated LODs for FAM, PAR, IND, and codrug were found to be  $3.076 \times 10^{-9}$ ,  $3.868 \times 10^{-10}$ ,  $1.066 \times 10^{-9}$ , and  $4.402 \times 10^{-9}$  mg/mL, respectively, while the calculated LOQs were  $9.322 \times 10^{-9}$ ,



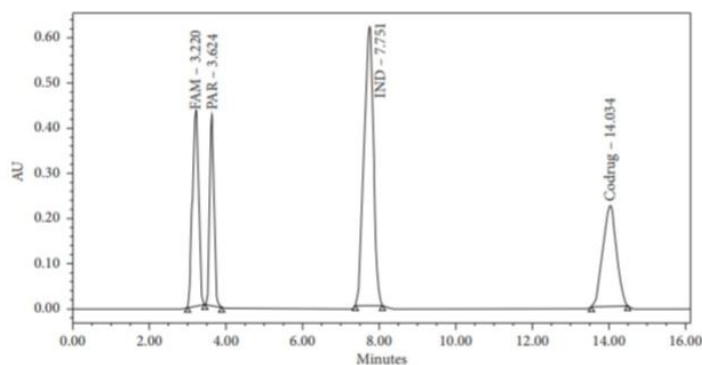


FIGURE 1: Chromatogram of the eluted peaks for the component mixture.

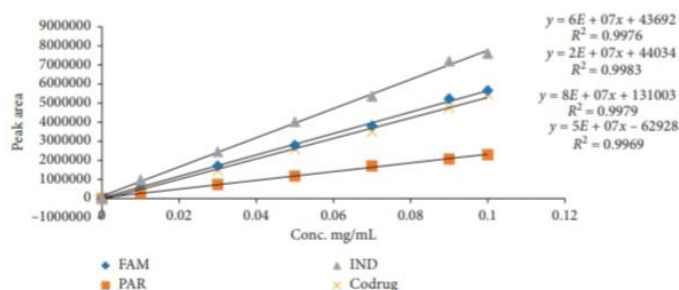


FIGURE 2: Linearity curves for compounds FAM, PAR, IND, and codrug.

$1.172 \times 10^{-10}$ ,  $3.232 \times 10^{-9}$ , and  $1.334 \times 10^{-8}$  mg/mL, respectively.

**3.3.6. Robustness.** Robustness is the capacity of a method to remain unaffected by minor variations in method conditions; in other words, it is a measure of the reliability of a method.

The robustness of an analytical procedure was tested by measuring its capacity of the developed method to remain unaffected by small but deliberate variations in the method parameters and providing an indication of its reliability during the normal use. For this study, the flow rate, wavelength, and pH parameters were changed for a mixture of 0.1 mg/mL. The results are summarized in Table 4. As can be observed, the % RSD values in all tested and varied parameters were less than 2.0 which indicates the good robustness of the developed analytical method. Moreover, the ANOVA test shows no significant difference for the tested compounds at different robustness validation parameters ( $p$  value  $>0.05$ ).

**3.3.7. System Suitability.** System suitability tests are utilized to justify that a system is performing sufficiently to guarantee confidence in the analytical method and the obtained results. The developed method showed that all of the standard system suitability parameters, including the resolution ( $R$ ), the symmetry of the peaks theoretical plates ( $N$ ), and retention factor ( $K$ ), are within acceptable limits as exhibited in Figure 4. The system suitability tests are summarized in Table 5.

An acidic mobile phase was used in the analytical method (pH = 5) and the results of the system suitability showed good results of the tested parameters indicating the method still performs very well under the acidic pH conditions. Moreover, the method was tested at lower pH (4.9) as a part of ruggedness and robustness validation, and results were not affected by this intended lowering of the mobile phase pH.

**3.4. In Vitro Hydrolysis of Codrug.** The developed analytical method was applied to investigate the *in vitro* conversion of the codrug to its parent drugs (IND and PAR) in the presence of esterase enzyme (1 U/mL) in PBS (pH 7) at 37°C.

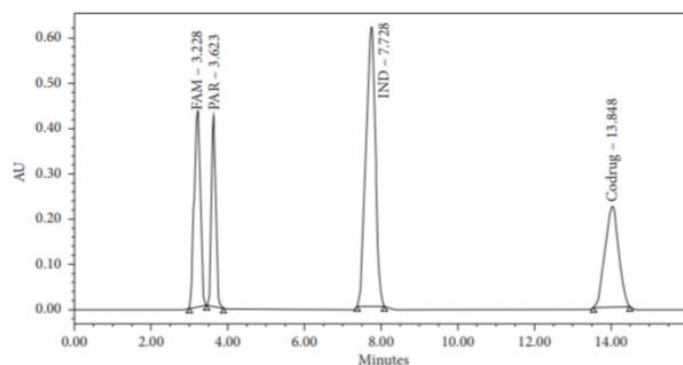


FIGURE 3: Chromatogram of the eluted peaks for the component mixture with inactive ingredients.

TABLE 2: The accuracy results in the concentration range (0.08–0.12 mg/mL).

Conc. (mg/mL)		FAM	PAR	IND	Codrug
0.08	Av. area	3070661.67	1868718.67	6561098.33	3306252.67
	% RSD	0.89	1.46	0.97	0.86
	% Recovery	99.34	100.76	100.73	99.5
0.1	Av. area	4294603.67	2347628.33	7736858.33	4166430.33
	% RSD	0.64	0.67	1.42	0.59
	% Recovery	99.5	99.98	99.22	101.38
0.12	Av. area	5238679.0	2886956.67	9774300	5300362.67
	% RSD	1.23	1.79	0.36	1.24
	% Recovery	100.33	100.89	100.88	100.82

TABLE 3: The precision results at different precision levels.

		FAM	PAR	IND	Codrug
System precision			0.1 (mg/mL)		
	Av. area	4227059	2314677	7742724	4178095
	% RSD	0.80	1.66	1.30	1.64
Intraday precision			0.08 (mg/mL)		
	Av. area	3147937	1904973	6560894	3288773
	% RSD	1.66	0.70	0.97	1.33
Interday precision			0.1 (mg/mL)		
	Av. area	4204444	2317970	7736858	4098577
	% RSD	0.76	1.75	1.42	0.20
Different analyst			0.12 (mg/mL)		
	Av. area	5249199	2878872	9739513	5286421
	% RSD	0.88	0.95	0.49	1.60

Without the esterase enzyme, the codrug is stable in PBS (pH 7) without the observation of any hydrolysis for one month. Upon the incubation with the esterase enzyme, a decrease in the codrug peak was observed with a concomitant increase

of IND and PAR HPLC peaks, and this conversion was quantified according to the developed equations. The complete conversion was observed after 60 min with a half-life of 12.2 min, as shown in Figure 5.

TABLE 4: Results of the robustness at different variable parameters.

		FAM	PAR	IND	Codrug
The wavelength of maximal absorption ( $\lambda_{max}$ )					
273 nm	Av. area	4279022	2357627	7713100	4191009
275 nm	Av. area	4225523	2324816	7797471	4109888
277 nm	Av. area	4263527	2374482	7759887	4186203
	% RSD	0.65	1.07	0.54	1.09
Mobile pH					
pH 5.1	Av. area	4353746	2280521	7609836	4089088
pH 4.9	Av. area	4355659	2247925	7803400	4177253
pH 5.0	Av. area	4225523	2324816	7797471	4109888
	% RSD	1.73	1.69	1.42	1.12
Flow rate					
Flow rate of 1.2 mL/min.	Av. area	4289108	2336035	7620148	4220573
Flow rate of 1.4 mL/min.	Av. area	4225523	2324816	7797471	4109888
	% RSD	1.06	0.34	1.63	1.88

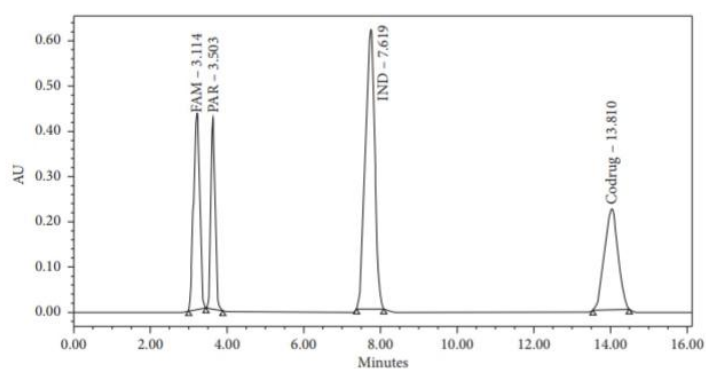
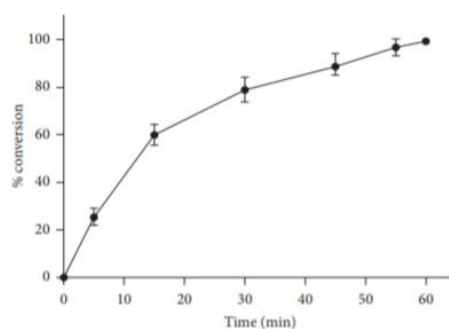


FIGURE 4: System suitability.

TABLE 5: System suitability.

	FAM	PAR	IND	Codrug
Resolution ( $R$ )	1.2	6.8	6.7	7.5
Symmetry of the peaks	1.1	0.9	1.1	1
Theoretical plates ( $N$ )	1418	2101	2160	6499
Retention factor ( $K$ )	1.67	2.08	5.41	10.42

FIGURE 5: *In vitro* hydrolysis of codrug in the presence of esterase enzyme (1 U/mL).

#### 4. Conclusion

In this study, IND and PAR codrug was successfully synthesized. RP-HPLC method was developed and validated according to the ICH Q2R1 and USP guidelines for the successful separation of a mixture containing four components formula: FAM, PAR, IND, and codrug. The tested parameters, including linearity, accuracy, selectivity, precision, limits of detection and quantification, and robustness, were found to be within the recommended guideline ranges. Moreover, the developed method was successfully applied to quantify the *in vitro* hydrolysis and conversion of codrug into its parent drugs. To the best of our knowledge, this is the first study that provides an easy and direct quantification method of a combination formula of different chemical compounds (FAM, PAR, IND, and codrug).

#### Data Availability

The data used to support the findings of this study are included within the article.

#### Conflicts of Interest

The authors declare that there are no conflicts of interest regarding the publication of this paper.

#### Acknowledgments

The authors would like to acknowledge the Faculty of Graduate Studies (master program of pharmaceutical sciences) at An-Najah National University for facilitating the accomplishment of the current work. The research did not receive any funding. The research was performed at An-Najah National University, Palestine.

#### References

- [1] M. C. Hochberg, R. D. Altman, K. T. April et al., "American college of rheumatology 2012 recommendations for the use of nonpharmacologic and pharmacologic therapies in osteoarthritis of the hand, hip, and knee," *Arthritis Care & Research*, vol. 64, no. 4, pp. 465–474, 2012.
- [2] H. Wen and K. Park, *Oral Controlled Release Formulation Design and Drug Delivery: Theory to Practice*, John Wiley & Sons, Hoboken, NJ, USA, 2011.
- [3] C. Sostres, C. J. Gargallo, M. T. Arroyo, and A. Lanas, "Adverse effects of non-steroidal anti-inflammatory drugs (NSAIDs, aspirin and coxibs) on upper gastrointestinal tract," *Best Practice & Research Clinical Gastroenterology*, vol. 24, no. 2, pp. 121–132, 2010.
- [4] K. Higuchi, E. Umegaki, T. Watanabe et al., "Present status and strategy of NSAIDs-induced small bowel injury," *Journal of Gastroenterology*, vol. 44, no. 9, pp. 879–888, 2009.
- [5] A. Lanas, M. Boers, and J. Nuevo, "Gastrointestinal events in at-risk patients starting non-steroidal anti-inflammatory drugs (NSAIDs) for rheumatic diseases: the EVIDENCE study of European routine practice," *Annals of the Rheumatic Diseases*, vol. 74, no. 4, pp. 675–681, 2015.
- [6] G. Sigthorsson, R. J. Simpson, M. Walley et al., "COX-1 and 2, intestinal integrity, and pathogenesis of nonsteroidal anti-inflammatory drug enteropathy in mice," *Gastroenterology*, vol. 122, no. 7, pp. 1913–1923, 2002.
- [7] M. Assali, M. Abualhasan, H. Sawafah, M. Hawash, and A. Mousa, "Synthesis, biological activity, and molecular modeling studies of pyrazole and triazole derivatives as selective COX-2 inhibitors," *Journal of Chemistry*, vol. 2020, Article ID 6393428, 14 pages, 2020.
- [8] K. C. Yeh, "Pharmacokinetic overview of indomethacin and sustained-release indomethacin," *The American Journal of Medicine*, vol. 79, no. 4, pp. 3–12, 1985.
- [9] E. Fritsche, S. J. Baek, L. M. King, D. C. Zeldin, T. E. Eling, and D. A. Bell, "Functional characterization of cyclooxygenase-2 polymorphisms," *Journal of Pharmacology and Experimental Therapeutics*, vol. 299, no. 2, pp. 468–476, 2001.
- [10] J.-L. Ziltener, S. Leal, and P.-E. Fournier, "Non-steroidal anti-inflammatory drugs for athletes: an update," *Annals of Physical and Rehabilitation Medicine*, vol. 53, no. 4, pp. 278–288, 2010.
- [11] S. Clarysse, D. Psachoulas, J. Brouwers et al., "Postprandial changes in solubilizing capacity of human intestinal fluids for BCS class II drugs," *Pharmaceutical Research*, vol. 26, no. 6, pp. 1456–1466, 2009.
- [12] O. Gallo, A. Franchi, L. Magnelli et al., "Cyclooxygenase-2 pathway correlates with VEGF expression in head and neck cancer. Implications for tumor angiogenesis and metastasis," *Neoplasia*, vol. 3, no. 1, pp. 53–61, 2001.
- [13] A. M. Farrag, "Synthesis and biological evaluation of novel indomethacin derivatives as potential anti-colon cancer agents," *Archiv der Pharmazie*, vol. 349, no. 12, pp. 904–914, 2016.
- [14] H. Matsui, O. Shimokawa, T. Kaneko, Y. Nagano, K. Rai, and I. Hyodo, "The pathophysiology of non-steroidal anti-inflammatory drug (NSAID)-induced mucosal injuries in stomach and small intestine," *Journal of Clinical Biochemistry and Nutrition*, vol. 48, no. 2, pp. 107–111, 2011.
- [15] A. Perez-Aisa, F. Sopena, E. Arceiz, J. Ortego, R. Sainz, and A. Lanas, "Effect of exogenous administration of transforming growth factor-beta and famotidine on the healing of duodenal ulcer under the impact of indomethacin," *Digestive and Liver Disease*, vol. 35, no. 6, pp. 397–403, 2003.
- [16] M. A. Hassan, M. S. Salem, M. S. Sueliman, and N. M. Najib, "Characterization of famotidine polymorphic forms," *International Journal of Pharmaceutics*, vol. 149, no. 2, pp. 227–232, 1997.
- [17] C. K. Ong, R. A. Seymour, P. Lirk, and A. F. Merry, "Combining paracetamol (acetaminophen) with nonsteroidal antiinflammatory drugs: a qualitative systematic review of analgesic efficacy for acute postoperative pain," *Anesthesia & Analgesia*, vol. 110, no. 4, pp. 1170–1179, 2010.
- [18] G. G. Graham and K. F. Scott, "Mechanism of action of paracetamol," *American Journal of Therapeutics*, vol. 12, no. 1, pp. 46–55, 2005.
- [19] G. G. Graham, M. J. Davies, R. O. Day, A. Mohamudally, and K. F. Scott, "The modern pharmacology of paracetamol: therapeutic actions, mechanism of action, metabolism, toxicity and recent pharmacological findings," *Inflammopharmacology*, vol. 21, no. 3, pp. 201–232, 2013.
- [20] A. N. Zaid, M. N. Abualhasan, N. Jaradat, M. Marar, K. Mansoor, and F. Qa'dan, "Development and validation of a new analytical HPLC method for the estimation of carvone in suppositories," *Journal of Pharmaceutical Investigation*, vol. 46, no. 2, pp. 557–563, 2016.
- [21] P. Seideman and A. Melander, "Equianalgesic effects of paracetamol and indomethacin in rheumatoid arthritis," *Rheumatology*, vol. 27, no. 2, pp. 117–122, 1988.



- [22] W. Schunack, "What are the differences between the H<sub>2</sub>-receptor antagonists?" *Alimentary Pharmacology & Therapeutics*, vol. 1, pp. 493s–503s, 2007.
- [23] Y. Naito, S. Iinuma, N. Yagi et al., "Prevention of indomethacin-induced gastric mucosal injury in helicobacter pylori-negative healthy volunteers: a comparison study rebamipide vs famotidine," *Journal of Clinical Biochemistry and Nutrition*, vol. 43, no. 1, pp. 34–40, 2008.
- [24] P. K. Sahu, N. R. Ramisetty, T. Cecchi, S. Swain, C. S. Patro, and J. Panda, "An overview of experimental designs in HPLC method development and validation," *Journal of Pharmaceutical and Biomedical Analysis*, vol. 147, pp. 590–611, 2018.
- [25] M. Assali, R. Shawahna, S. Dayyeh, M. Shareef, and I.-A. Alhimony, "Dexamethasone-diclofenac loaded polylactide nanoparticles: preparation, release and anti-inflammatory activity," *European Journal of Pharmaceutical Sciences*, vol. 122, pp. 179–184, 2018.
- [26] I. H. T. Guideline, "Text on validation of analytical procedures," in *International Conference on Harmonization*, Geneva, Switzerland, 1994.
- [27] I. S. Committee, "ICH harmonised tripartite guidelines. Validation of analytical procedures: methodology Q2," in *Proceedings of the International Conference on Harmonisation of Technical Requirements for Registration of Pharmaceuticals for Human Use*, Geneva, Switzerland, 1996.
- [28] USP-36, Buffer solutions in united states pharmacopeia, second supplement to USP36–NF31, p. 6244, 2013.
- [29] P. Ravisankar, C. N. Navya, D. Pravalika, and D. N. Sri, "A review on step-by-step analytical method validation," *IOSR Journal of Pharmacy*, vol. 5, no. 10, pp. 7–19, 2015.
- [30] M. N. Abualhasan, "A validated stability-indicating HPLC method for routine analysis of an injectable lincomycin and spectinomycin formulation," *Scientia Pharmaceutica*, vol. 80, no. 4, pp. 977–986, 2012.
- [31] M. Assali, M. Joulani, R. Awwad et al., "Facile synthesis of ciprofloxacin prodrug analogues to improve its water solubility and antibacterial activity," *ChemistrySelect*, vol. 1, no. 6, pp. 1132–1135, 2016.
- [32] M. Assali, N. Kittana, S. A. Qasem et al., "Combretastatin A4-camptothecin micelles as combination therapy for effective anticancer activity," *RSC Advances*, vol. 9, no. 2, pp. 1055–1061, 2019.
- [33] M. Assali, A. N. Zaid, N. Kittana, D. Hamad, and J. Amer, "Covalent functionalization of SWCNT with combretastatin A4 for cancer therapy," *Nanotechnology*, vol. 29, no. 24, Article ID 245101, 2018.
- [34] ICH, Guideline, ICH harmonized tripartite: validation of analytical procedures: text and methodology, 2005.
- [35] M. Abualhasan, M. Ghanem, M. Assali, and A. Zaid, "The effect of non-compliance of PPI instruction on the stability of reconstituted oral antibiotics," *Journal of Applied Pharmaceutical Science*, vol. 5, no. 8, pp. 143–146, 2015.
- [36] M. Abualhasan, M. Assali, N. Jaradat, and T. Sarhan, "Synthesis, formulation and analytical method validation of rutin derivative," *Letters in Drug Design & Discovery*, vol. 16, no. 6, pp. 685–695, 2019.

جامعة النجاح الوطنية  
كلية الدراسات العليا

تحضير جزيئات نانوية متعددة المكونات للعلاج الفعال المضاد  
للالتهابات الغير جرثومية

إعداد

نهال زياد عزت زهد

إشراف

د. محي الدين العسالي

قدّمت هذه الأطروحة استكمالاً لمتطلبات الحصول على درجة الماجستير في العلوم الصيدلانية،  
بكلية الدراسات العليا، في جامعة النجاح الوطنية، نابلس - فلسطين.

2020

ب

تحضير جزيئات نانوية متعددة المكونات للعلاج الفعال المضاد للالتهابات الغير جرثومية

إعداد

نهال زياد عزت زهد

إشراف

د. محي الدين العسالي

الملخص

**الخلفية:** الأدوية المضادة للالتهابات غير الستيرويدية (NSAIDs) هي من بين الأدوية الأكثر شيوعًا والموصوفة على نطاق واسع لكل من الألم والالتهاب. ومع ذلك، فإن سمعتهم السيئة في إحداث تأثيرات معدية معوية، وقلة الذوبان في الماء وقصر فترة عمر النصف لديها واللدان سيؤثران على رضا المريض وعلى الامتصاص عن طريق الفم لهم وبالتالي هذا يبرر الحاجة إلى مضادات الالتهاب غير الستيرويدية بطريقة إطلاق متحكم بها ومستمرة. في الآونة الأخيرة، تعتبر تقنية الجسيمات النانوية تقنية ذكية للتغلب على هذه العيوب. في هذه الأطروحة، فقد قمنا بتطوير أنظمة نانوية لتوصيل عدة أدوية وهي: إندوميثاسين، باراسيتامول وفاموتيدين باستخدام تقنيات مُستحلب النانوي والجسيمات النانوية البوليمرية.

**المنهجية:** بدءًا من تصنيع الدواء الثنائي المُركَّب من الإندوميثاسين والباراسيتامول والمرتبطة برابطة إستر قابلة للتحلل متبوعة بالتحميل المُسبق لهذا الدواء المُركَّب في مستحلب نانوي (Co-NE) والذي سيتم تحميله في جزيئات نانوية بوليمرية مختلفة تحتوي على دواء فاموتيدين باستخدام نهج الترسيب النانوي. تم فحص نُظُم النانو المُطَوَّرة عن طريق المجهر الإلكتروني، وانتثار الضوء الديناميكي وتحليل جهد زيتا. علاوة على ذلك، تم اختبار دراسة الاستقرار والتوافق الحيوي. بالإضافة إلى ذلك، تم تطوير طريقة RP-HPLC جديدة والتحقق من صحتها وفقًا لإرشادات ICH من أجل دراسة شكل التَّحرير في المختبر للأدوية المُحمَّلة (FAM والكودراج).

**النتائج:** أظهرت هذه النظم النانوية المطورة حجمًا هيدروديناميكيًا بين 190-240 نانومتر وتتراوح القيم المحتملة للزيتا من -30 إلى -48 مللي فولت. أكدت صور TEM تحميل Co-NE في جزيئات نانوية بوليمرية مختلفة. وكشفت دراسات الاستقرار أن هذه النظم النانوية كانت مستقرة عند درجات حرارة مختلفة و في بيئة كيميائية تحتوي محاليل منظمة لدرجة الحموضة على مدى شهر واحد. علاوة على ذلك، فإن تحسين قابلية الذوبان لهذه الأدوية الثلاثة باستخدام تقنية التغليف هذه يؤدي إلى الحصول على إطلاق متحكم به للأنظمة متعددة المكونات وهي الدواء الثنائي المركب Co-drug وفاموتيدين على مدى ثلاثة أيام. بالإضافة إلى القياس الكمي للأدوية الأربعة على تشغيل HPLC واحد من خلال التطوير والتحقق من طريقة RP-HPLC، وقد تم استخدامها بنجاح لتحديد كمية التحلل المائي في المختبر وإطلاقه وتحميله وتحويله.

**الخلاصة:** هذه الجسيمات النانوية متعددة المكونات قد تكون منصة محتملة للتغلب على عقبات مضادات الالتهاب غير الستيروئيدية، وتآزر الأدوية بآليات مختلفة من الإجراءات من خلال المشاركة في تغليف مستحلب نانوي صغير الحجم في داخل ناقلات نانوية بوليمرية مختلفة لغرض الوصول إلى هدف العلاج الفعال المضاد للالتهابات غير جراثومية.

